

# PERFORMANCE EVALUATION OF OPTICAL BURST-MODE RECEIVERS

BY

GAO YAN

A THESIS

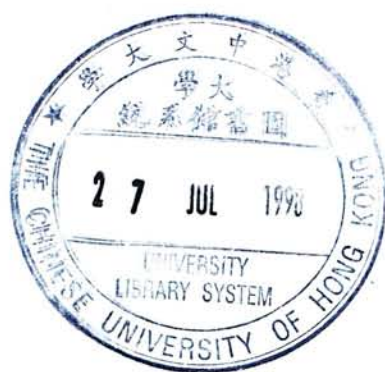
SUBMITTED IN PARTIAL FULFILLMENT OF THE REQUIREMENTS

FOR THE DEGREE OF MASTER OF PHILOSOPHY

DIVISION OF INFORMATION ENGINEERING

THE CHINESE UNIVERSITY OF HONG KONG

Printed: September 22, 1997



# Acknowledgement

I would like to express my deep gratitude to my supervisor, Prof. Kwok-wai Cheung, for his full support and guidance during my two-years' study in Hong Kong. Professor Cheung is an expert in the field of lightwave communication system and device technology. He has enlightened me on the field of communication networks and given me much valuable advice and comments on my research. His scholarship, wisdom, and sincerity toward work impressed me greatly and will definitely benefit me in my future career.

I also wish to express my appreciation to Prof. L. K. Chen and Prof. F. K. Tong. They have taught me a lot of knowledge as well as given me a lot of help and encouragement.

I would like to thank my colleges in the lightwave communication lab and some staff in the Information Engineering Division. They all have provided me much precious help and assistance. They are Dr. C. K. Chan, Mr. Y. H. Wang, Dr. C. Su, Mr. W. H. Siu, Mr. K. W. Ko, Mr. S. F. Lam, Miss W. S. Chan, Mr. L. C. Wong, Mr. K. L. Lo, Dr. Q. L. Ding, Mr. W. Jiang, Miss J. Yao, Dr. X. L. Guo, Dr. X. Li, Mr. A. Qin, Mr. J. H. Chan.

Last but not least, I am indebted to my husband and my parents for their constant support and various sacrifices.

# Abstract

Burst-mode receivers play an important role in high-speed all-optical multiaccess packet networks because they can quickly recover the packet data. They can also be used in local loop distribution and copper-based networks.

A practical burst-mode receiver was first realized by Ota and Swartz for high-speed optical data transmission systems. It is a DC-coupled burst-mode optical receiver with an automatic threshold control circuit. A few preamble bits are attached before each burst packet to determine the detection threshold for that packet. Thus the detection threshold can be set adaptively according to the amplitude of the incoming bursts. However, a sensitivity penalty, with respect to the continuous mode receivers having a fixed threshold, exists in the burst-mode receivers. Eldering pointed out a sensitivity penalty owing to the corruption of threshold by noise. Su et al. revealed that another origin of the penalty was due to the threshold decay during the data reception process. This thesis looks further into the investigation of bit error rate (BER) performance by Su et al. and put forward the problem of choosing an optimal detection threshold, aiming to improve the performance in burst-mode receiver.

Currently the detection threshold in a burst-mode receiver is always set halfway between symbols "1" and "0", just as in a continuous-mode receiver.



Since the adaptive threshold control circuit employs a natural charging and discharging mechanism, after the detection threshold has been established in the preamble field of the packet, the threshold will decay when “0” bits are present in the subsequent payload data. Thus we argue that the detection threshold should be selected at an optimal position between “1” and “0” instead of the midpoint in order to minimize the BER. The optimal threshold depends on both the decay parameter of the burst-mode receiver and the signal to noise ratio of the incoming data packets. By setting the threshold at the optimal level instead of setting at halfway between the bits “1” and “0”, BER can be improved. Accordingly the sensitivity penalty with respect to the continuous-mode receiver is reduced.

This paper also looks into an MLT-3 burst-mode receiver, as MLT-3 is a three-level coding standardized for high speed data transmission over unshielded twisted-pair (UTP) cable. A schematic of burst-mode receiver that is suitable for MLT-3 signaling is proposed in this thesis. Based on the effect of threshold decay the BER performance of MLT-3 burst-mode receiver are evaluated. Similar to the case in binary signaling, a BER degradation is observed and a sensitivity penalty is produced compared to the MLT-3 continuous-mode receiver. An optimal threshold is also chosen to optimize the BER performance in MLT-3 burst-mode receiver.

# Contents

<b>1</b>	<b>Introduction</b>	<b>1</b>
1.1	Background . . . . .	1
1.2	Purpose of Study . . . . .	5
1.3	Organization of Chapters . . . . .	7
<b>2</b>	<b>Overview of Optical Burst-Mode Receivers</b>	<b>8</b>
2.1	Introduction . . . . .	8
2.2	Burst-Mode Data Transmission . . . . .	9
2.3	Two Main Issues on Burst-Mode Receiver . . . . .	11
2.4	Model of Burst-Mode Receiver . . . . .	13
2.5	Threshold Detection in Burst-Mode Receiver . . . . .	16
2.6	Sensitivity Penalty in Burst-Mode Receiver . . . . .	20
2.7	Chapter Summary . . . . .	22
<b>3</b>	<b>Optimal Detection Threshold in Burst-mode Receiver</b>	<b>24</b>
3.1	Introduction . . . . .	24
3.2	Threshold Fluctuation in Burst-Mode Receiver . . . . .	25
3.3	BER of Burst-Mode Receiver . . . . .	27

3.4	Optimal Detection Threshold of Burst-Mode Receivers . . . . .	31
3.5	Simulation Result on the BER of Burst-mode Receiver . . . . .	36
3.6	Chapter Summary . . . . .	38
<b>4</b>	<b>MLT-3 Burst-Mode Receiver</b>	<b>41</b>
4.1	Introduction . . . . .	41
4.2	MLT-3 Line Code . . . . .	42
4.3	BER Performance of MLT-3 Continuous-Mode Receiver . . . . .	45
4.4	Burst-mode Receiver For MLT-3 Line Code . . . . .	49
4.5	BER Performance of MLT-3 Burst-Mode Receiver . . . . .	52
4.6	Chapter Summary . . . . .	55
<b>5</b>	<b>Conclusion</b>	<b>59</b>
	<b>Bibliography</b>	<b>62</b>

# List of Figures

1.1	A PON network transmit burst and packet data . . . . .	4
2.1	Signal formats used in digital optical communications . . . . .	10
2.2	Block diagram of traditional continuous-mode receiver . . . . .	13
2.3	A schematic of feedback burst-mode receiver . . . . .	14
2.4	A feedforward burst-mode receiver . . . . .	16
2.5	Threshold detection in traditional continuous-mode receiver . .	17
2.6	The circuit of peak detector . . . . .	18
2.7	The circuit of a modified peak detector . . . . .	19
3.1	Threshold fluctuation in a burst-mode receiver . . . . .	26
3.2	BER versus the threshold parameter $R$ under $\text{SNR}=21.6\text{dB}$ . . .	32
3.3	Optimal threshold parameter $R_p$ versus the decay parameter $k$ under $\text{SNR}=21.6\text{dB}$ and $\text{SNR}=24.1\text{dB}$ . . . . .	34
3.4	Comparison of BER versus the decay parameter $k$ when $R = R_p$ and $R = 0.5$ under $\text{SNR}=21.6\text{dB}$ , Solid line corresponds to $R =$ $R_p$ while dashed line corresponds to $R = 0.5$ . . . . .	35
3.5	Optimal threshold parameter $R_p$ versus $\text{SNR}$ at $k = 0.05$ , $k =$ $0.10$ and $k = 0.15$ . . . . .	36



3.6	Bit error rate versus SNR at $k = 0.05$ and $k = 0.10$ . Solid lines are the optimized BER, dashed lines are the BER when $R = 0.5$	37
3.7	Sensitivity penalty versus the decay parameter $k$	38
3.8	Simulation diagram of BER performance for burst-mode receiver	39
3.9	Simulation results of BER versus decay parameter when $SNR = 21.6dB$ . Little circles represent the simulation results, solid line represents the theoretical result.	40
4.1	MLT-3 coding of sample stream	43
4.2	MLT-3 transition state diagram	44
4.3	NRZI and MLT-3 coding a stream of "1"s	45
4.4	Probability density functions for MLT-3 transmission over additive Gaussian noise channel	46
4.5	BER versus SNR in MLT-3 code	48
4.6	Schematic diagram of MLT-3 burst-mode receiver	49
4.7	Threshold variation of MLT-3 burst-mode receiver	51
4.8	Optimal threshold parameter $R_p$ versus the decay parameter $k$ under $SNR=21.6dB$ and $SNR=24.1dB$ in MLT-3 burst-mode receiver	54
4.9	Optimal threshold parameter $R_p$ versus the signal SNR at $k=0.05$ and $k=0.10$ in MLT-3 burst-mode receiver	55
4.10	BER versus the decay parameter $k$ when $R = R_p$ under $SNR=21.6dB$ in MLT-3 burst-mode receiver	56
4.11	BER versus SNR when $k = 0.05$ and $k = 0$ in MLT-3 burst-mode receiver	57



4.12 Sensitivity penalty versus  $k$  to maintain a BER of  $10^{-9}$  in MLT-3

burst-mode receiver . . . . .	58
-------------------------------	----

# Chapter 1

## Introduction

### 1.1 Background

Fiber-optic communication systems employ optical fibers for information transmission and have revolutionized the field of communications. The development of optical transmission systems progressed very rapidly in the latter half of the 1970s with the advent of the important technologies such as low-loss optical fibers and long-life semiconductor lasers. The first commercial optical transmission system was introduced in the first half of the 1980s.

Now fiber-optic communications are already being used in several distinct fields of applications such as submarine transmission systems, telephone networks, computer networks, cable television networks, etc. Nowadays they are universally recognized to have wide potential applications in many other domains.

In principle, the signal bandwidth in optical communication systems can exceed 1 THz because of the high capacity offered by the optical fibers. However,

in practice, it is often limited to 10 Gb/s or less because of electronic-speed limitations and fiber dispersion. It is difficult to realize the electrical circuit if the transmission bit rate exceeds 10Gb/s. The use of multiple channels over the same fiber provides a simple way to utilize the unprecedented capacity offered by optics. Optical time division multiplexing (TDM) [1], soliton transmission, and dense wavelength division multiplexing (WDM) or optical frequency division multiplexing (FDM) [2] are promising candidates for constructing larger capacity and flexible photonic networks.

Research has concentrated on Wavelength Division Multiplexing (WDM) where the wavelength of the light is used as a degree of freedom to route the signals using optical selection (filtering) stages. The use of wavelength has been extensively investigated for both closed user broadcast networks as well as single and multi-hop transport networks. Present research on the scalability of such approaches focuses on the issues such as spectral dependence of the amplifier gain, fiber nonlinearities, such as Stimulated Raman Scattering(SRS) and Four-Wave-Mixing(FWM), and the limits imposed on the number of wavelength channels and the transmission distance.

Alternatively, Time Division Multiplexing (TDM) can be employed. This approach uses a single wavelength to carry data. Such systems base on a clock frequency and tributary data rates which are easily accessible using electronic components. Short optical pulses are used in a Return-to-Zero (RZ) data transmission format with temporal interleaving to map a number of optical data channels into a single electronic clock cycle.

To utilize the transmission capacity offered by optical fibers. It is also desirable to share the available fiber bandwidth between several communication

nodes by allowing multiple access to the same resource. By taking advantage of the beneficial properties offered by optics multiple access to the same resource, these new networks make it possible to circumvent the electronic bottlenecks.

Multiple access can be accomplished by multiplexing several communication nodes in either spectral domain or time domain. In spectral domain, one can distinguish wavelength division multiple access (WDMA) and subcarrier multiple access (SCMA). In time domain, two implementation approaches can be distinguished: time division multiple access (TDMA) and code division multiple access (CDMA).

Now there is a wide consensus that multiaccess passive optical networks (PON's) will provide the basis for cost-effective penetration of fiber systems into the local networks [4, 5]. In the PON distribution networks, the path between the central office (CO) and the subscribers is passive and optical: no opto-electronic nor electro-optic conversion is performed except at the ends of the connection. PON's can provide high capacity to support the increasing information loads of various service demand.

A PON architecture is shown in Fig.1.1. The signal streams destined to and sent from several subscribers are multiplexed onto a single fiber to the CO. Typically, a passive optical splitter is used to broadcast the multiplexed signal from the CO to the subscribers (a bus topology using passive optical taps or any other passive-broadcast fiber-network topology can be used as well). Upstream transmission, from the subscribers to the CO, requires a multiaccess scheme to combine the signals in a noninterfering way. TDMA is currently considered a very attractive candidate for such a purpose [6, 7, 8].

In TDMA, each node shares the communication resources by sending data in



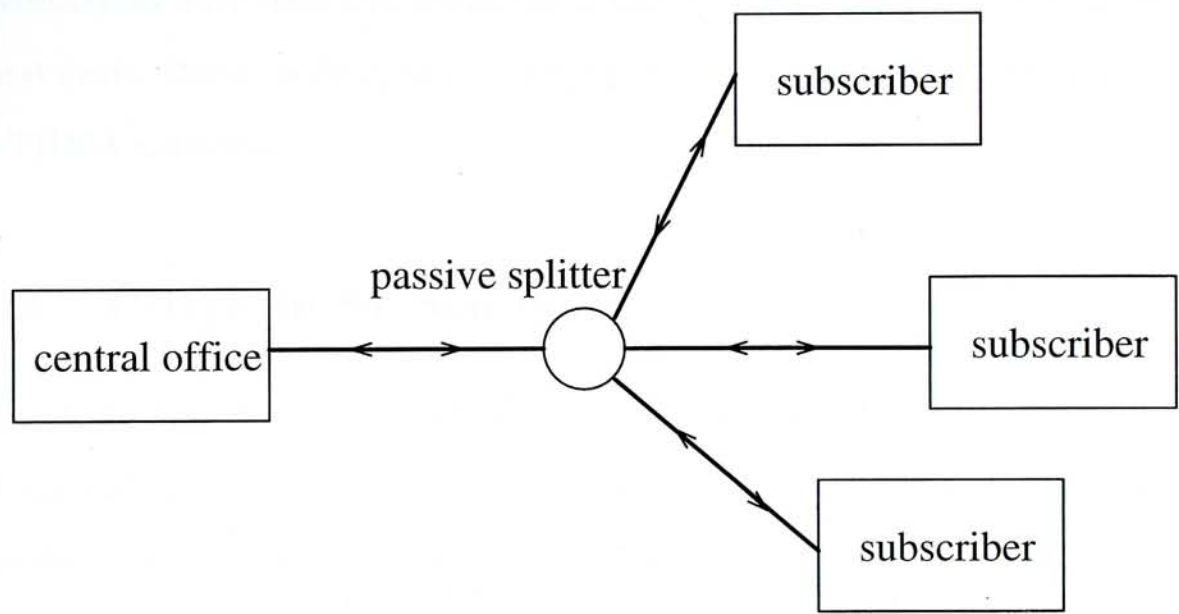


Figure 1.1: A PON network transmit burst and packet data

a synchronized way in order to avoid data collision. In contrast to conventional point-to-point links, a very significant feature of these all-optical multiaccess networks is that the amplitude and the phase of the received packets can be quite different from packet to packet due to different attenuation for different length of fiber and different chromatic dispersion caused by the variation in transmitters' wavelengths. The amount of amplitude and phase variations between two bursty data packets can be as high as 20 dB and 360 degrees, respectively. Hence, these definitely lead to serious problems during data receptions, since it is difficult for a receiver at one node to retrieve the bursty data with different amplitudes and phases from other nodes. Conventional receivers are not suitable for burst-mode data reception because it cannot instantaneously handle the arriving packets



with large differences in both optical power and arriving time. It is therefore necessary to have receivers which can adapt to these variations on a burst-by-burst basis. Burst-mode optical receiver is thus a very important building block in TDMA networks.

## 1.2 Purpose of Study

Ota et al. first designed a high-speed, burst-mode digital compatible receiver for optical bus or packet communications [9, 10]. It employed an automatic threshold tracking level control circuit and a dc-coupled decision circuit. The threshold control circuit can capture data amplitude and set the logic threshold in about 1 ns. Using an avalanche photodiode, the typical receiver sensitivity is -37.5 dBm ( $BER = 10^{-9}$ ) at bit rates up to 900Mb/s, and with a dynamic range of 23 dB for both pseudo-random and burst-mode signals. But obviously, this kind of digital burst-mode receivers has a sensitivity penalty with respect to continuous-mode optical receivers.

Eldering [12] studied the origin of this penalty and claimed that it was induced by the noise corrupted threshold (NCT). He concluded that this sensitivity penalty decreases as the number of bits used to establish the threshold increases. Su et al. [13] pointed out that Eldering's analysis was incomplete. He stated that not only the noise will corrupt the detected threshold, but also the detected threshold itself will decay whenever the incoming signal bit is "0". This threshold decay definitely induces a sensitivity penalty. Thus Su et al. gave a more complete and unified theory for the performance of burst-mode receiver [14].

In the above performance evaluation on burst-mode receiver, we observed

that the detection threshold is always set at the halfway level between bit "1" and bit "0" after detecting the level of bit '1' in preamble field. This is the traditional practice in continuous-mode receiver to get the best BER performance. However as the threshold will decay during the bit "0" in the information data field, the optimal threshold for burst-mode receiver should not be the mean level between bit "1" and "0" again. Therefore, this thesis is to study the performance of burst-mode receivers and find out the optimal detection threshold to reduce the BER. It was found that when using the optimal detection threshold instead of the halfway between bit "1" and "0" level, the BER can be reduced when other conditions remain the same.

Recently, there has been more and more demand on high speed data transmission over unshielded twisted-pair (UTP), the TP-PMD group has chosen a three-level coding scheme called MLT-3 to run FDDI protocols on UTP. This line code is chosen to meet the requirements of the electron-magnetic interference when high speed data is transmitted. Moreover, this multi-level line code can also be employed for data transmission with other protocols, where the transmission media is band-limited or higher system transmission capacity is required. If the MLT-3 signaling is used in multiaccess networks, burst-mode receivers that can deal with this kind of multi-level signal is required to be developed.

In this thesis the BER performance of MLT-3 receivers in both continuous mode and burst mode are examined. It's shown that the decay parameter  $k$  of the threshold will also decay the performance of MLT-3 burst-mode receivers. As the decay parameter  $k$  increases, a larger sensitivity penalty is required to obtain the same BER. Our proposed optimal detection threshold can also be used to reduce this penalty.

### **1.3 Organization of Chapters**

This thesis consists of five chapters. Chapter 1 introduces the application of optical burst-mode receiver and the focus of this thesis. Chapter 2 gives an overview of optical burst-mode receiver. Chapter 3 investigates the performance of binary optical burst-mode receivers and proposes that the detection threshold should be set at an optimal value to obtain the better BER performance. Chapter 4 describe a schematic of burst-mode receiver for multi-level MLT-3 signaling, and discusses about the performance of continuous-mode and burst-mode receiver receiving MLT-3 signals. Chapter 5 is the conclusion of this thesis.



## Chapter 2

# Overview of Optical Burst-Mode Receivers

### 2.1 Introduction

Optical burst-mode receiver plays a very important role in all-optical multiaccess networks which can provide high transmission speed and fast packet switching to support multimedia services. In this chapter we will first introduce the concept of burst-mode data transmission, then interpret the two main issues on burst-mode receiver, and describe the models of burst-mode receiver. Next, we will look into the peak detector (adaptive threshold control circuit) which is a key part in a burst-mode receiver followed by the analysis of two different schemes for threshold detection. Finally, the sensitivity penalty of burst-mode receiver with respect to continuous-mode receiver will be investigated.

## **2.2 Burst-Mode Data Transmission**

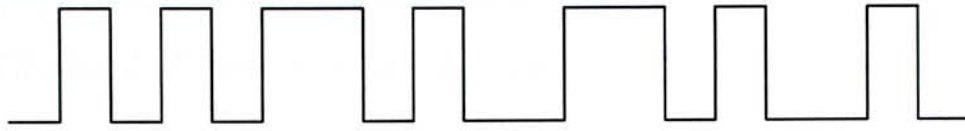
In traditional optical point-to-point communication systems, the signal transmission is always in a synchronous or iso-synchronous way. Once the communication link between the two ends is established, information will be continuously sent from the transmitter to the receiver. Even when the system is in an idle state, an extra synchronous signal should be transmitted to maintain the system's synchronization. In addition, in order to guarantee the synchronization, a line code is usually used to provide enough clock information for both data and clock recovery. This kind of signal transmission is called continuous-mode data transmission.

In the communication networks with multiaccess protocols, packets transmission and switching techniques are usually used. Such networks can support both synchronous and asynchronous data transmissions. The transmitters can be turned off when they are in an idle state. This technique provides great flexibility and high efficiency in information transmission.

Moreover, in these multipoint systems based on TDMA, different distances between several nodes result in different packet amplitudes in the receiver, and the decision threshold used in the detector for digital level restoration must be modified from burst to burst. Therefore, in this kind of networks, packet transmission with multiaccess protocols will lead to burst-mode data transmission which is different from the continuous-mode transmission.

Ota et al.[15] described three types of signal formats in digital optical communications as shown in Fig.2.1. Pattern (1) is known as the continuous mode data. The binary sequence is continuously sent with an approximately balanced

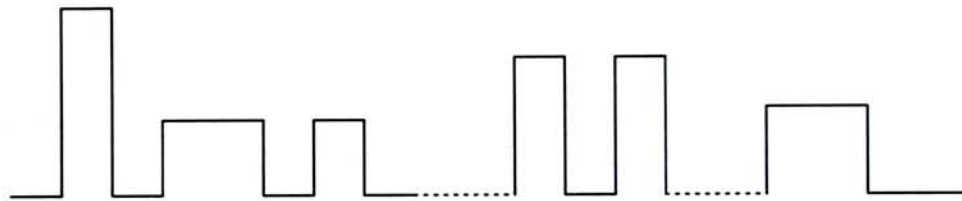




(1) Continuous mode data



(2) Burst mode data



(3) Burst and packet mode data

Figure 2.1: Signal formats used in digital optical communications

ratio of “1”s and “0”s, and the maximum interval between any two logic transitions is strictly limited. Examples are the nBmB line codes commonly used in point-to-point link applications.

Pattern (2) is defined as burst-mode data, in which the ratio of “1”s to “0”s and the interval between logic transitions are not constrained. The sequences have the same amplitude for the same logic symbol. The low speed data using RS-232 in computers follows this pattern.

In the case of pattern (3), the signal amplitude may vary from packet to packet and a guard time is usually used between two packets from different nodes. This kind of data is referred as burst and packet mode data. It often appears in multiaccess packet transmission networks.

In this thesis, when we mention about burst-mode data transmission, we refer to the data transmission of both patterns (2) and (3). The task for a burst-mode receiver is to recover the data of both patterns (2) and (3) correctly and quickly.

## **2.3 Two Main Issues on Burst-Mode Receiver**

For burst-mode data transmission in multiaccess packet networks, the packets transmitted from different nodes will propagate through different distances and thus experience different losses. There are dead spaces of uncertain length between these packets. Hence it is not easy for the receiver to recover the amplitudes and phases of the incoming bursty packets within a very short time. The two main issues need to be considered in optical burst-mode receiver are phase recovery and amplitude recovery.

Quick recovery of the clock phase of each burst is essential. Traditional ways to recover the clock (frequency or phase) of received data are by means of narrow-band pass filters (NBPF) or narrow-band phase locked loop (PLL). These techniques based on narrow-band circuitries work effectively for the acquisition of clock information in continuous-mode data transmission. However, they are insufficient for burst-mode data operation, because they need a large number of preamble bits in the packet to “warm up” the receiver, it will lead to a large

degradation for the channel utilization in burst-mode data transmission.

Several ways to achieve instantaneous clock synchronization for burst-mode data have been proposed. They are

- global clock with correlator for phase detection [16];
- quenched narrowband tank circuit [17];
- gated-oscillators with PLL [18].

Among the above techniques, the last one is the most promising method as it can provide fast clock and phase recovery within one bit duration, which results in negligible capacity penalty. In addition, the circuitry is suitable for high level circuit integration because of its simplicity.

Amplitude recovery in burst-mode receiver is also different from that in continuous-mode because the packets emitted by different nodes will impinge the receiver with different optical power. The receiver thus requires a large dynamic range to adapt to the variations in power on a burst-to-burst basis. An automatic threshold detection circuit is very essential in the configuration of a burst-mode receiver.

To conduct synchronization and power leveling, a preamble field of several bits are added at the beginning of each burst-mode packet. The preamble field consists of an amplitude recovery field, which allows the receiver to adapt to different received optical power; and a clock recovery field, which allows the receiver to extract the timing information from the burst. In view of the transmission efficiency, it is desirable to keep the length of preamble field as short as possible in multiaccess packet networks.



## 2.4 Model of Burst-Mode Receiver

There is a fundamental difference between the traditional continuous-mode receiver and the new burst-mode receiver. Here for comparison, we will first briefly overview the operation of a traditional receiver.

Fig.2.2 shows the block diagram of a conventional optical receiver [19]. The photo-detector first converts the optical input into an electrical signal, then the signal is amplified by the preamplifier for subsequent processing. After that the received signal enters a post-amplifier with an automatic gain control (AGC) circuit for further amplifying. The low-pass filter after the post-amplifier is used to equalize the signal waveform and reduce the noise. The resulting amplified signal is fixed at an adequate amplitude which is independent of the input optical power at the receiver. At last a comparator with a fixed threshold level can be used to determine the binary data sequence.

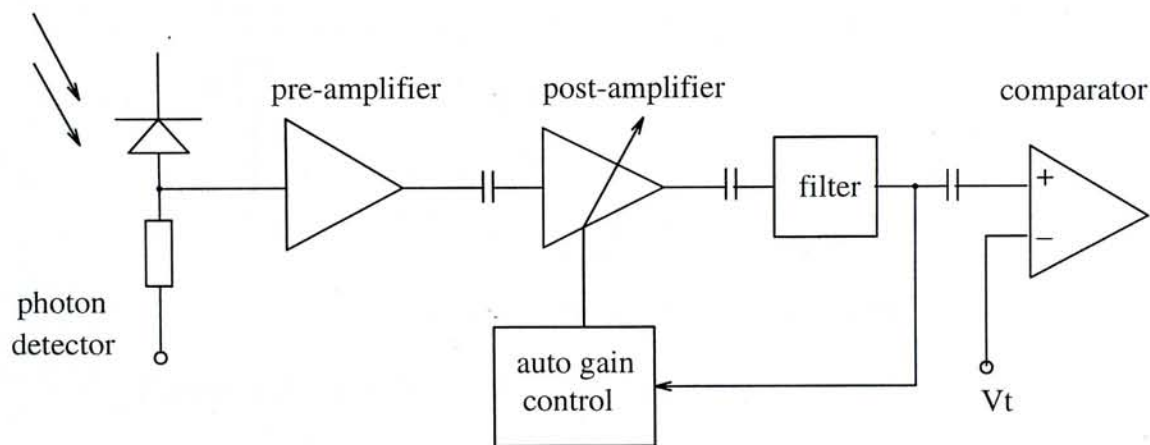


Figure 2.2: Block diagram of traditional continuous-mode receiver

It is easy to see that in a conventional receiver, the signal path is AC-coupled thus the signal's low frequency component is filtered out. The advantage is that a high sensitivity can be achieved. However, as there is a charge and discharge time for capacitors as well as the slow response time of AGC in the circuitry, the average amplitude of the input data is not allowed to vary rapidly in a short time. Therefore this kind of receivers is not suitable for receiving the burst-mode data.

The burst-mode receiver is DC-coupled and the threshold setting for the circuitry must adapt to the amplitudes of received burst signal within a very short time. Also the clock and phase recovery of a burst-mode receiver must be performed very quickly.

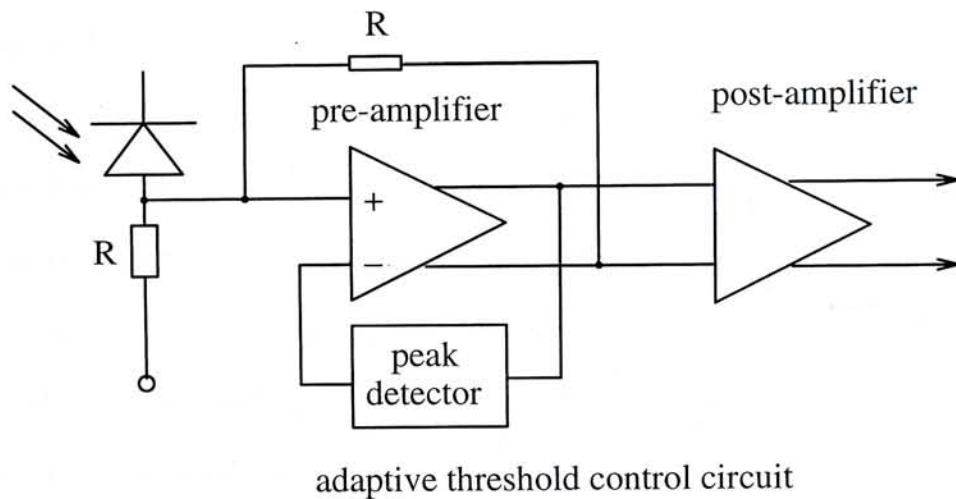


Figure 2.3: A schematic of feedback burst-mode receiver

Ota et al. proposed a schematic of burst-mode receiver shown in Fig.2.3 [9]. The preamplifier uses a differential input/output trans-impedance amplifier with



transimpedance  $R$ . The peak detector (threshold level control circuit) consists of an operational amplifier peak hold capacitor, and a divider network and forms a negative feedback loop between the output and input of preamplifier. The peak detector determines the instantaneous detection threshold of the incoming signal. The output of the pre-amplifier is DC-coupled to a differential post-amplifier for further amplification. When a signal current is applied to the input of preamplifier, the peak detector creates a reference voltage of exactly half of the signal output, that is, the product of the photocurrent and transimpedance.

The receiver was assembled in a compact dual in-line package with an optical connector. The typical sensitivities are around -31.5 and -29.5 dBm/Av at 200 Mb/s (at bit error rate of  $10^{-9}$ ) for continuous-mode and burst-mode signals, respectively, with dynamic ranges of 27.5 and 25.5 dB, respectively. The operating bit rate ranges from dc to 500 Mb/s and the differential outputs are true emitter coupled logic (ECL).

Another type of burst-mode receiver which has a feedforward structure is described by Eldering [12], shown in Fig.2.4. In the above feedback type receiver, the signal's amplitude recovery is performed in the preamplifier, while in this scheme, it is done in the post-amplifier. The received signal is first amplified by the pre-amplifier and then split into two branches. One branch is DC-coupled to a differential amplifier, another is feedforward into a peak detector to extract the amplitude information of received packets. From the output of the peak detector, a proper threshold level can be adaptively set in front of the differential post-amplifier.

As far as the hardware implementation is concerned, the operation of the feedback structure enables the receiver to work more reliable, thus is more stable

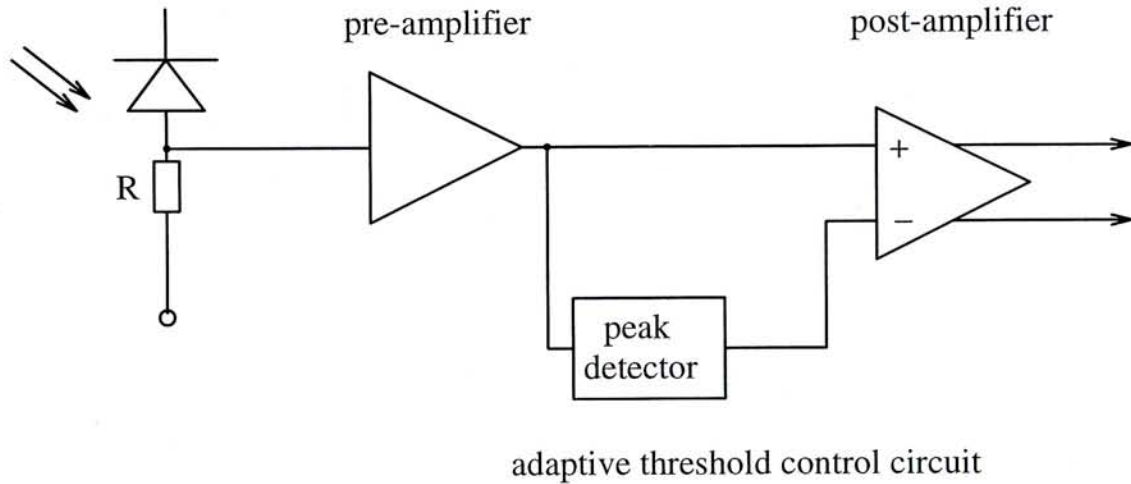


Figure 2.4: A feedforward burst-mode receiver

than the feedforward structure. However, a differential input/output preamplifier is needed in the former whereas a conventional DC-coupled pre-amplifier can be used for the latter.

## 2.5 Threshold Detection in Burst-Mode Receiver

In the optical digital receiver, usually the incoming signal is a train of pulses whose waveform is distorted after filtering by the transmission channel. If the input to this channel is a two-level digital signal, the amplitude of each of them must take one of the two possible values, “1” or “0”. The noisy signal is compared with a given threshold. It is decided as “1” when the symbol is larger than the threshold, and as “0” when it is smaller.

In traditional continuous-mode receiver, the detection threshold is achieved

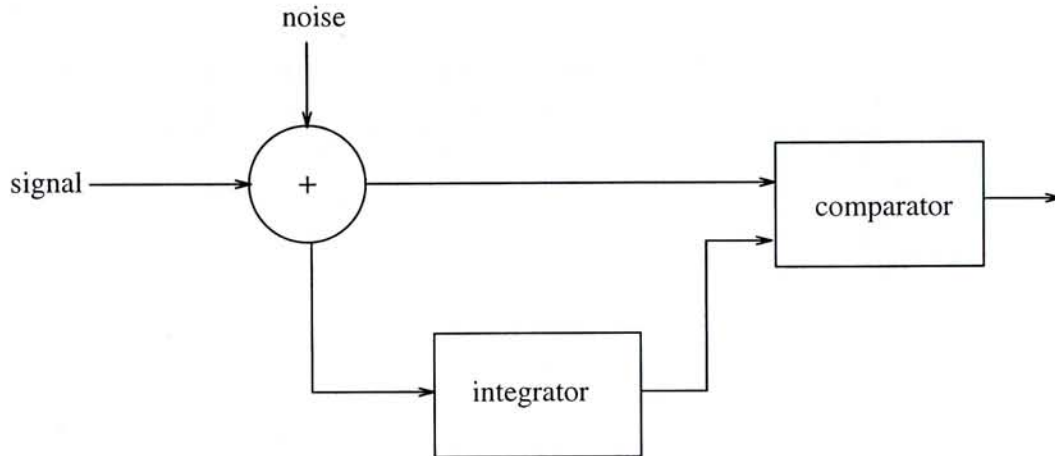


Figure 2.5: Threshold detection in traditional continuous-mode receiver

by averaging the input signal as shown in Fig.2.5. When the integration time is very long (ideally infinite), the integrator can provide a constant and noise-free threshold directly used for detection. In binary signal transmission the probability of both symbols is identical, the output amplitude of the integrator is halfway between bit “1” and “0”.

In burst-mode data transmission, it is not possible to conduct continuous integration on the input data. Thus a preamble field consisting of several symbol “1”s is required to be added at the beginning of each burst for the purpose of establishing the threshold prior to the payload data transmission. Here the work of threshold determination and holding is completed by a circuit called peak detector.

The circuit of peak detector is shown in Fig.2.6. The capacitor in the circuit will be charged during the preamble field before the payload data. A proper



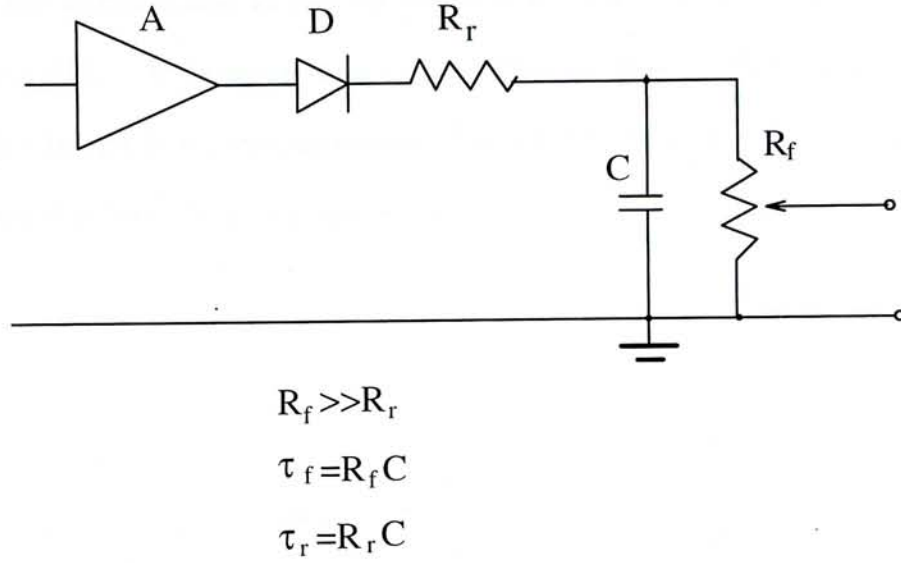


Figure 2.6: The circuit of peak detector

threshold then is established through the use of a simple voltage divider at the output. The charge and discharge time constant of the capacitor are denoted as  $\tau_r$  and  $\tau_f$  respectively, given by

$$\begin{aligned}
 \tau_r &= R_r C \\
 \tau_f &= R_f C
 \end{aligned} \tag{2.1}$$

usually  $R_r \ll R_f$ . There are two different ways in choosing the resistances, resulting in two different schemes for threshold detecting and holding in the peak detector circuit.

One scheme simply employs a natural charge and discharge mechanism on the capacitor [10]. After the threshold amplitude is acquired from the preamble field preceding the payload in each data packet, the data stream itself can also affect



the threshold amplitude. The discharge time constant must be set large enough to avoid the threshold from decaying seriously when there are long stream of zeros. But on the other hand it has to be smaller than the dataless guard time between packets [12]. A large guard time between the packets will lead to a capacity penalty in network transmission. Under this schematic the charge time constant  $\tau_r$  lasts for less than one bit period.

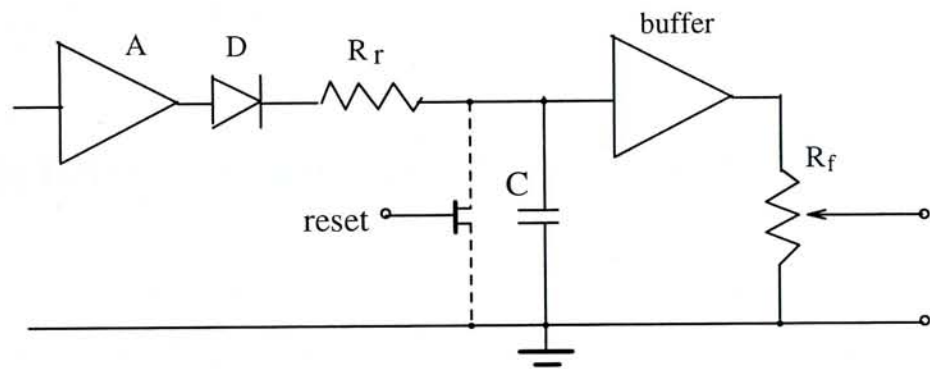


Figure 2.7: The circuit of a modified peak detector

Another schematic [12] has a little variation from the previous one, shown in Fig.2.7. The discharge time constant is set to approach infinity by isolating the divider network with a high input impedance buffer. At the end of each burst a reset pulse activates a fast discharge through an analog gate. This allows the peak detector to get ready for the next data packet without prolonging the guard time between packets. This circuit has the advantage that once the capacitor is fully charged in the preamble field prior to the data field, the threshold amplitude can be kept unvaried during the subsequent long chain of

zeros. Also here the charge time constant can be chosen to correspond to several bits of the preamble, not necessarily less than one bit.

The first scheme has the advantage of simplicity and is compatible with traditional continuous-mode receiver. In the second scheme, the threshold reset mechanism can be used in fixed-size packet transmission by counting the number of bits in a packet [20]. For variable-sized packets, unique frame-start and frame-end symbols must be used to encapsulate the packets to trigger the reset and detect process. This encoding will lead to another capacity penalty for data transmission. Thus it may not benefit from employing such scheme.

## **2.6 Sensitivity Penalty in Burst-Mode Receiver**

In optical binary signal reception, the received noisy signal is compared with the reference threshold to determine whether it is “1” or “0”. The performance criterion for the receiver is governed by the bit-error rate (BER), which is defined as the probability of incorrect identification of a bit by the decision circuit of the receiver. A commonly used criterion for digital optical receivers requires a BER of less than  $10^{-9}$ . The receiver sensitivity is then defined as the minimum average received power required by the receiver to operate at a BER of  $10^{-9}$ .

The continuous-mode receiver has a fixed detection threshold. In burst-mode receiver, the decision threshold is determined from the receiving signals by the peak detector. The BER is therefore degraded as the symbol decision is made by comparing the input to a reference level which is no longer fixed. This introduces an intrinsic sensitivity penalty with respect to continuous-mode receivers.

One origin of this penalty is that the preamble bits used to establish the



decision threshold are corrupted by noise [12, 22]. Eldering first addressed this problem and determined numerically the penalty caused by reception noise in the peak detector as a function of the number of bits used for threshold detection. It is suggested that by properly choosing the charge time constant for the peak detector, it is possible to make the charge time correspond to the  $n$  bits of the preamble. Thus the peak detector can act as an integrator for averaging the detected threshold of the  $n$ -bit consecutive "1"s in the preamble, and the variance for the detected threshold can decrease by  $n$  times. Therefore, the ambiguity of the detected threshold can be reduced. From the computation, it is shown that when one, four, eight bits are used for the measurement of the threshold, there are 3dB, 0.94dB and 0.5dB power penalty respectively for the burst-mode receiver with respect to the continuous-mode receiver. With a slow rising time constant in the peak detection circuitry and a large number of preamble bits for the threshold detection, the receiver will have a better performance.

Another inherent sensitivity penalty exists in a burst-mode receiver employing the first type of peak detector presented in Fig.2.6. The threshold decays in the subsequent payload field after having been established. This decay is inevitable because the adaptive threshold control circuit (peak detector) uses a natural charge and discharge mechanism. The threshold cannot be kept constant but fluctuating according to the incoming data pattern. Whenever a bit "0" comes, the threshold will decay because of the intrinsic characteristic of the adaptive threshold control circuit. Thus when there are consecutive "0"s in the signal sequence, the threshold decay will be quite large, causing a considerable degradation in the receiver's BER. Su et al. investigated this problem and proposed theoretical analysis and simulation results [13]. Also a unified model

for burst-mode receivers considering both the above origins of the sensitivity penalty was presented [14].

## **2.7 Chapter Summary**

Optical fiber applications in LAN, WAN and intercomputer communications are, in most cases, characterized by transmissions of burst-mode data, in which the data packets have different amplitudes and phases with dataless spaces. In these communication systems burst-mode receivers have to be used instead of the traditional continuous-mode ones. Fast amplitude recovery and phase recovery are the two main issues in the design of burst-mode receivers. A preamble field is normally added to the beginning of each bursty packet to realize burst-mode reception.

The fundamental differences between the two kinds of receivers are that DC-coupling must be used throughout the burst-mode receiver instead of AC-coupling. According to their structure, burst-mode receivers can be classified into feedback type and feedforward type. As far as the adaptive threshold control circuit (peak detector) of the burst-mode receiver is concerned, there are two schemes for threshold detecting and holding by choosing different circuit constants. One is to let the threshold charge and discharge with the incoming signal adaptively, the other is to detect the threshold from the preamble field then hold constantly during the payload field. Since the detection threshold in burst-mode receiver is not fixed as in the continuous-mode receiver, there is a sensitivity penalty in burst-mode receiver. One cause is that the detected threshold has been corrupted by noise. Another cause comes from the fluctuation of



the threshold when detecting the data signal.

## Chapter 3

# Optimal Detection Threshold in Burst-mode Receiver

### 3.1 Introduction

In the last chapter we have mentioned that one origin of the sensitivity penalty in burst-mode receivers with respect to continuous-mode receivers is that the threshold is not fixed but decays during the reception of digital data. In this chapter, we will first investigate the threshold fluctuation in the process of data decision, and give an expression of bit error rate (BER) for burst-mode receiver. Then we focus on optimizing the BER performance by setting an optimal detection threshold in the receiver. The analysis shows that by choosing an optimal threshold instead of the halfway between symbol “1” and “0” for binary signals, the BER of the burst-mode receivers can be improved under the same conditions, and the sensitivity penalty can be reduced accordingly. The analysis is also verified by computer simulation.

### 3.2 Threshold Fluctuation in Burst-Mode Receiver

In a burst-mode receiver using an adaptive threshold control circuit, the detection threshold varies with the instantaneous amplitude of the incoming signals as shown in Fig.3.1. Firstly the threshold is detected from the preamble field (consists of all “1” bits) and adjusted properly for detecting the subsequent data. But, during the signal detection period, when the incoming bit is “0”, the threshold will be discharged to a lower level. On the contrary, when the incoming bit is “1”, the threshold will be recharged to the preset level. The charge time constant of the circuit is often set very small in order that the threshold can recover to the preset level quickly. Meanwhile the discharge time constant has to be carefully set. If it is too small, the threshold will decay rapidly and the performance of the receiver will degrade seriously. If it is too large, a large gap time between two consecutive burst packets is needed and a large transmission capacity penalty will be resulted [23].

Fig.3.1 represents the voltage of the incoming data of a burst-mode receiver, the threshold voltage can be represented as a function of the charge time constant and discharge time constant. After the detection threshold is established at the end of the preamble field, the instantaneous threshold can be expressed by a Markov process as follows

$$V[m, t] = \begin{cases} V[m-1, T]e^{(-t/\tau_f)} & a(m) = \text{“0”} \\ V[m-1, T] + (V_T - V[m-1, T])(1 - e^{-t/\tau_r}) & a(m) = \text{“1”} \end{cases} \quad (3.1)$$

where  $V[m, t]$  is the threshold voltage at time  $t$  in the  $m$ -th bit,  $t$  is measured with respect to the start of each bit period,  $0 \leq t \leq T$  with  $T$  being the

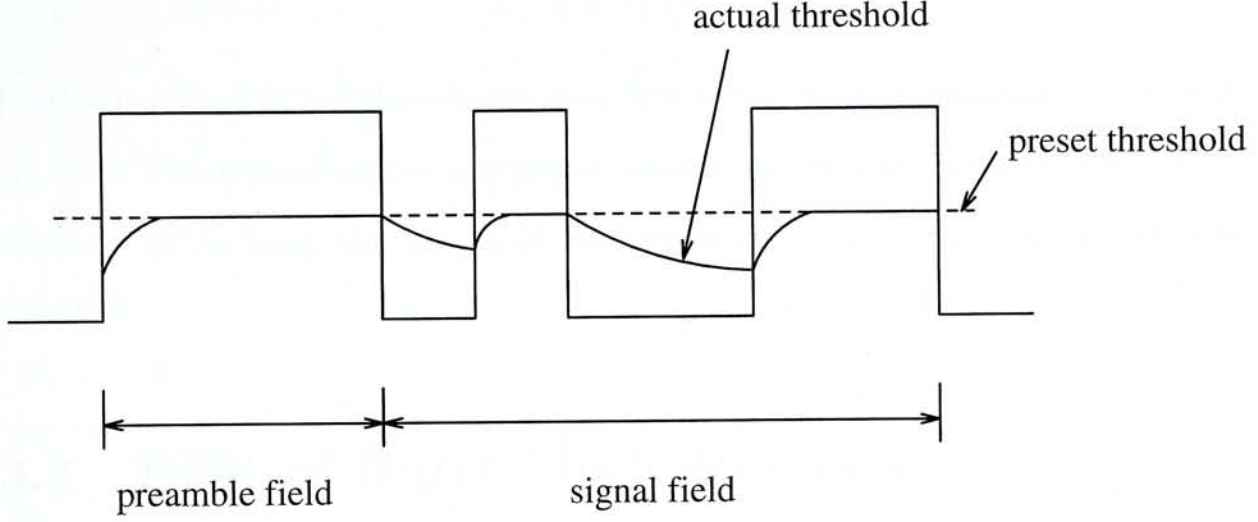


Figure 3.1: Threshold fluctuation in a burst-mode receiver

duration of each bit,  $m$  is counted from the start of the signal field,  $\tau_f$  and  $\tau_r$  are the discharge (holding) time and charge (rising) time constant of the adaptive threshold control circuit respectively,  $a(m)$  is the symbol ("0" or "1") for the  $m$ -th bit, and  $V_T$  is the preset threshold voltage detected from the preamble field. The voltage level for symbol "0" is taken to be zero for simplicity.

In digital receiver, to minimize the bit error rate probability, symbol detection usually takes place at the center of each bit period, i.e.,  $t = T/2$ , where the eye opening is maximum. When there is a string of consecutive "0"s present in the input signal, the instantaneous detection threshold  $V_{T0j}$  for the  $j$ th "0" bit in the consecutive "0" sequence is given by

$$V_{T0j} = V[m, T/2] = V_T e^{-(j-1/2)k} \quad (3.2)$$



where  $k$  is the decay parameter defined as

$$k = T/\tau_f. \quad (3.3)$$

From equation (3.2), if the current data symbol is “0”, the instantaneous threshold for it will depend on the number of consecutive “0”s preceding the bit. If the chain of “0” is long, the threshold will seriously deviate from the initial value  $V_T$ .

### 3.3 BER of Burst-Mode Receiver

The bit error rate (BER) of the binary continuous-mode receiver can be expressed as

$$BER = P(1)P(0/1) + P(0)P(1/0) \quad (3.4)$$

where  $P(1)$  and  $P(0)$  are the probabilities of receiving “1” and “0”, respectively,  $P(1/0)$  is the probabilities of deciding of a logical “0” when “1” is received, and  $P(0/1)$  is the probability of deciding of a logic “1” when “0” is received.

In a pulse-code modulated (PCM) bit stream “1” and “0” are equally likely to occur, so that  $P(1)=P(0)=1/2$ . Both  $P(0/1)$  and  $P(1/0)$  depend on the probability density function of the received signals. The functional form depends on the statistics of noise sources responsible for signal fluctuations. For usual receivers based on pin-photodetectors followed by high impedance or transimpedance preamplifiers, additive white Gaussian noise limits the receiver sensitivity. So we can assume the signal noise complies with Gaussian distribution with zero mean and variance  $\sigma^2$ . Then the probabilities are given by

$$P(0/1) = \frac{1}{\sigma_1\sqrt{2\pi}} \int_{-\infty}^{V_T} \exp\left[-\frac{(V - V_1)^2}{2\sigma_1^2}\right] dV$$

$$P(1/0) = \frac{1}{\sigma_0\sqrt{2\pi}} \int_{V_T}^{\infty} \exp\left[-\frac{(V - V_0)^2}{2\sigma_0^2}\right] dV \quad (3.5)$$

where  $V_1$  and  $V_0$  are the voltages for bit “1” and “0” respectively,  $V_T$  is the threshold preset at the receiver,  $\sigma_1$  and  $\sigma_0$  are the root-mean-square (RMS) noise for bit “1” and “0”. In receivers implemented with pin-photodetectors and high impedance or transimpedance preamplifiers, thermal-noise considerably exceeds shot noise. Therefore the additive perturbation is independent of the signal, which means  $\sigma_1 = \sigma_0 = \sigma$ . Then the BER is given by

$$\begin{aligned} BER &= \frac{1}{2} \left\{ \frac{1}{\sigma\sqrt{2\pi}} \int_{-\infty}^{V_T} \exp\left[-\frac{(V - V_1)^2}{2\sigma^2}\right] dV + \frac{1}{\sigma\sqrt{2\pi}} \int_{V_T}^{\infty} \exp\left[-\frac{(V - V_0)^2}{2\sigma^2}\right] dV \right\} \\ &= \frac{1}{2} \left[ \operatorname{erfc}\left(\frac{V_1 - V_T}{\sigma}\right) + \operatorname{erfc}\left(\frac{V_T - V_0}{\sigma}\right) \right] \end{aligned} \quad (3.6)$$

where  $\operatorname{erfc}(x)$  stands for the complementary error function defined as

$$\begin{aligned} \operatorname{erfc}(x) &= \frac{1}{\sqrt{2\pi}} \int_x^{\infty} e^{-z^2/2} dz \\ &\approx \frac{1}{x\sqrt{2\pi}} e^{-x^2/2}. \end{aligned} \quad (3.7)$$

Equation (3.6) shows that BER depends on the decision threshold  $V_T$ , which can be optimized to minimize the BER. The minimum occurs when  $V_T$  is chosen that

$$\frac{V_1 - V_T}{\sigma} = \frac{V_T - V_0}{\sigma} = Q. \quad (3.8)$$

An explicit expression for  $V_T$  is

$$V_T = \frac{V_1 + V_0}{2} \quad (3.9)$$

which means the decision threshold  $V_T$  is placed at the midpoint between  $V_1$  and  $V_0$ .

The BER with optimum setting of decision threshold is then given by

$$\begin{aligned} BER &= \operatorname{erfc}(Q) \\ &\approx \frac{1}{Q\sqrt{2\pi}} e^{-Q^2/2} \end{aligned} \quad (3.10)$$

where  $Q$  is obtained by

$$Q = \frac{V_1 - V_0}{2\sigma}. \quad (3.11)$$

A typical system requirement is to obtain a BER of  $10^{-9}$  and this corresponds to  $Q = 6$ . The BER can also be related to the signal to noise ratio (SNR). By noting that

$$SNR = \frac{(V_1 - V_0)^2}{\sigma^2} \quad (3.12)$$

we have

$$BER = \operatorname{erfc}\left(\frac{\sqrt{SNR}}{2}\right). \quad (3.13)$$

SNR must be at least 144 or 21.6dB for achieving  $BER \leq 10^{-9}$ . The corresponding optical power needed is the receiver sensitivity.

The BER consideration is different in burst-mode receiver. The detection threshold will decay according to the incoming signal level because of the nature of the adaptive threshold control circuit.  $V_T$  in equation (3.5) and (3.6) is not constant, but data pattern dependent.

When the incoming signal is “1”, the instantaneous detection threshold  $V_{T1}$  in burst-mode receiver is approximately equal to  $V_T$  in continuous-mode receiver, so  $P(0/1)$  can be regarded the same as in continuous-mode receiver. When the incoming signal is “0”, the instantaneous threshold  $V_{T0}$  will decay from  $V_T$  to a smaller value by equation (3.2), that will increase  $P(1/0)$  and finally degrade the BER of burst-mode receiver.



For a length of  $i$  consecutive “0”s in the data stream, the average error probability for the  $i$  consecutive “0”s can be expressed as

$$P_{ei} = P_i \cdot \frac{1}{i} \sum_{j=1}^i P(1/0)_j \quad (3.14)$$

where  $P_i$  is the probability of  $i$  consecutive “0”s present in the data stream, and  $P(1/0)_j$  is the error probability for the  $j$ th “0” in the chain.

In a pseudo-random input signal sequence with length of  $N = 2^n - 1$ , the probability of  $i$  “0” bits appearing consecutively is  $1/2^{i+1}$ . Thus the average BER for burst-mode receiver can be expressed as

$$BER = \frac{1}{2}P(0/1) + \sum_{i=1}^n \frac{1}{2^{i+1}} \frac{1}{i} \sum_{j=1}^i P(1/0)_j \quad (3.15)$$

where

$$P(0/1) = \frac{1}{\sigma\sqrt{2\pi}} \int_{-\infty}^{V_{T1}} \exp\left[-\frac{(V - V_1)^2}{2\sigma^2}\right] dV$$

$$P(1/0)_j = \frac{1}{\sigma\sqrt{2\pi}} \int_{V_{T0j}}^{\infty} \exp\left[-\frac{(V - V_0)^2}{2\sigma^2}\right] dV. \quad (3.16)$$

In the above equations,  $V_{T1} = V_T$ ,  $V_{T0j} = V_T e^{-(j-1/2)^k}$  from Section 2.4.1, and we have already assumed  $\sigma_1 = \sigma_0 = \sigma$ .

If we define

$$Q_1 = \frac{V_1 - V_{T1}}{\sigma}$$

$$Q_{0j} = \frac{V_{T0j} - V_0}{\sigma} \quad (3.17)$$

and using the complementary error function  $\text{erfc}(x)$ , equation (3.15) can be rewritten as

$$BER = \frac{1}{2}\text{erfc}(Q_1) + \sum_{i=1}^n \frac{1}{2^{i+1}} \frac{1}{i} \sum_{j=1}^i \text{erfc}(Q_{0j})$$



$$\approx \frac{1}{2} \frac{\exp(-Q_1^2/2)}{\sqrt{2\pi}Q_1} + \sum_{i=1}^n \frac{1}{2^{i+1}} \frac{1}{i} \sum_{j=1}^i \frac{\exp(-Q_{0j}^2/2)}{\sqrt{2\pi}Q_{0j}}. \quad (3.18)$$

### 3.4 Optimal Detection Threshold of Burst-Mode Receivers

In a binary continuous-mode receiver, the detection threshold is usually placed midway between the amplitude of bit “1” and “0” to achieve the best BER performance. But in burst-mode receiver, since the threshold will decay during the signal bit stream, the average level of the threshold will be less than the threshold which is initially preset. In such a situation we can tell intuitively that the optimal detection threshold will not be the halfway between “1” and “0” any more.

It is reasonable to claim that if the detection threshold is preset higher than the halfway between “1” and “0”, it may compensate part of the threshold decay and improve the BER. Of course, the threshold level cannot be set too high, otherwise the error probability of receiving bit “1” will increase and the overall BER of the receiver will not get better. There should exist an optimal level of the detection threshold. If the threshold is placed at this optimal level instead of the halfway, the BER degradation of the burst-mode receiver will be reduced, and therefore the performance of the receiver can be improved.

For the convenience of the following analysis, a weighting factor is used to relate the amplitude of detection threshold to the amplitude of the signal. We

define the threshold parameter  $R$ ,

$$R = \frac{V_T - V_0}{V_1 - V_0}. \quad (3.19)$$

$R$  falls in the range between 0 and 1, i.e.,  $0 < R < 1$ . Different  $R$  corresponds to different threshold position between amplitude of bit "1" and bit "0". When  $V_T$  is set at the halfway between  $V_1$  and  $V_0$ ,  $R$  equals to 0.5. Here we denote  $R_p$  as the optimal threshold parameter when the minimum BER can be achieved.  $V_{Tp}$  is the optimal detection threshold, it can be obtained from  $R_p$  by

$$V_{Tp} = R_p \cdot (V_1 - V_0) + V_0 \quad (3.20)$$

Thus to find an optimal  $V_{Tp}$  is equivalent to find  $R_p$ .

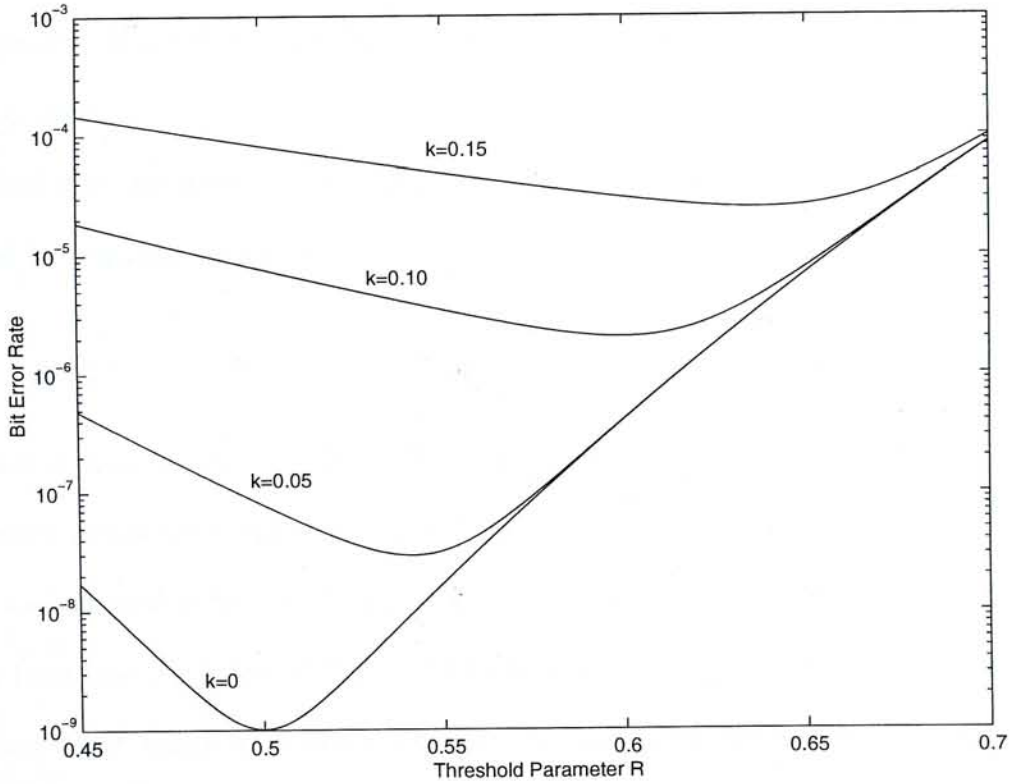


Figure 3.2: BER versus the threshold parameter  $R$  under  $\text{SNR}=21.6\text{dB}$

From Equation (3.17), (3.18), (3.20), (3.2) and (3.12), we can obtain BER

as a function of R

$$BER = \frac{1}{2} \frac{\exp(-(1-R)^2(SNR)^2/2)}{\sqrt{2\pi}(1-R)(SNR)} + \sum_{i=1}^n \frac{1}{2^{i+1}} \frac{1}{i} \sum_{j=1}^i \frac{\exp(-(SNR)^2 e^{-2(j-1/2)k}/2)}{\sqrt{2\pi}(SNR)e^{-(j-1/2)k}} \quad (3.21)$$

where SNR is the peak-to-peak signal to noise ratio, k is the decay parameter. Here we have assumed the On-Off Keying (OOK) signal has a good extinction ratio, so that  $V_0$  is taken as zero.

This relationship is shown graphically in Fig.3.2, where SNR is 144 or 21.6 dB and k is set at different values. We take n as 15 for the pseudo-random sequence. In the figure the curve  $k = 0$  actually represents the BER in a continuous-mode receiver, whose optimal threshold parameter is 0.5 and the optimized BER is  $10^{-9}$ . In the case of burst-mode receiver, the optimal threshold parameter  $R_p$  is always greater than 0.5 and a BER penalty exists with respect to the continuous-mode receiver.

To find the optimal threshold parameter  $R_p$  to achieve the minimum BER, R should be chosen to satisfy

$$\frac{d(BER)}{dR_p} = 0. \quad (3.22)$$

This is an equation that is difficult to obtain the close form solution. So we use a computer numerical calculation to find out  $R_p$ .

The calculated value of  $R_p$  has dependence on both k and SNR. Fig.3.3 shows  $R_p$  as a function of k for  $SNR = 21.6dB$  and  $SNR = 24.1dB$ . From the figure we can see that when k becomes larger,  $R_p$  deviates farther from 0.5.

Fig.3.4 compares the receiver's BER performance at the optimal threshold and the midway threshold between "1" and "0" when k varies under a fixed SNR. The BER can be obviously improved by setting the threshold at the optimal



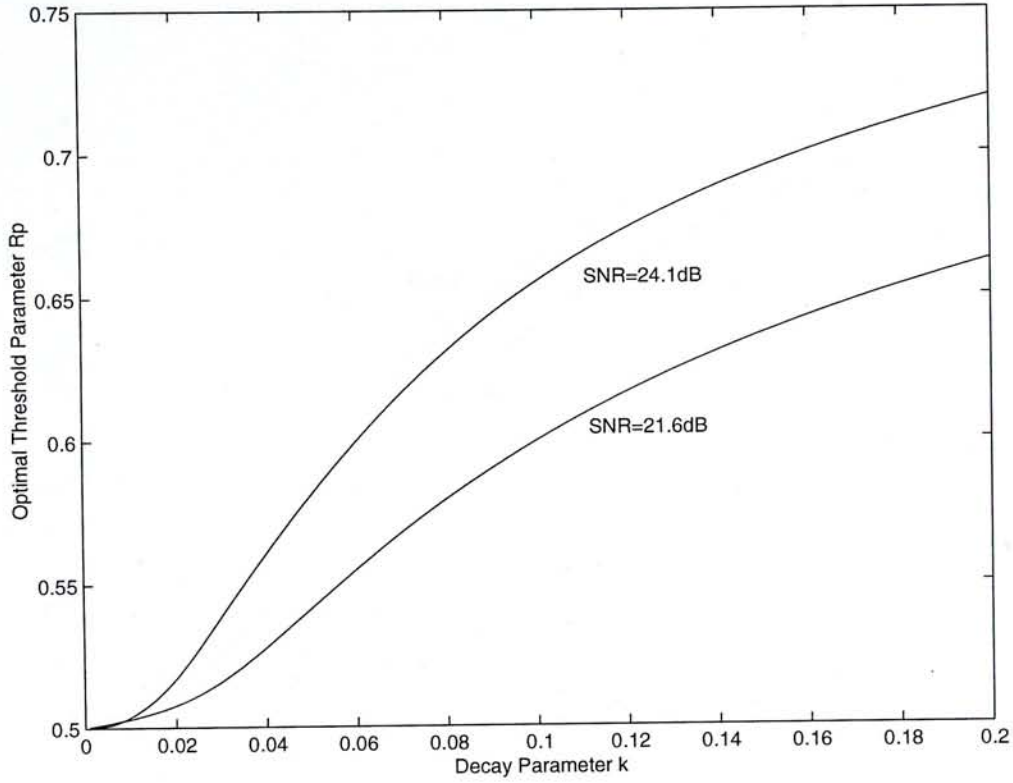


Figure 3.3: Optimal threshold parameter  $R_p$  versus the decay parameter  $k$  under SNR=21.6dB and SNR=24.1dB

value. Also it is clearly shown that under the same SNR, even the BER in burst-mode receiver is optimized by choosing the optimal threshold, it still has a penalty compared to the continuous-mode receiver ( $k = 0$ ). And this BER penalty becomes larger as  $k$  becomes larger.

The optimal threshold parameter  $R_p$  also depends on the signal to noise ratio SNR. Fig.3.5 shows the relationship when  $k = 0.05$ ,  $k = 0.10$  and  $k = 0.15$ .  $R_p$  increases as SNR increases. For each couple of values of SNR and  $R_p$  at  $k = 0.05$  and  $k = 0.10$ , the BER is computed for different SNR and is shown in Fig.3.6. where BER computed from  $R = 0.5$  are also drawn in dashed lines for reference.

To achieve the same BER performance, a burst-mode receiver has a sensitivity penalty with respect to the continuous-mode receiver. Fig.3.7 shows the

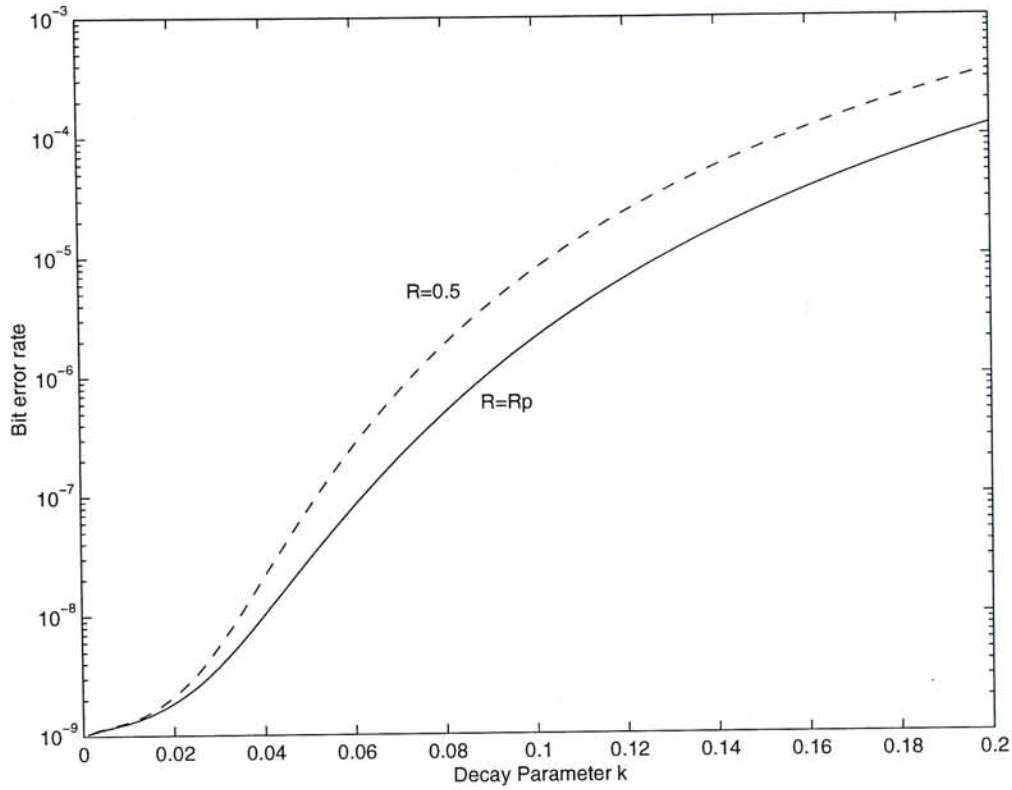


Figure 3.4: Comparison of BER versus the decay parameter  $k$  when  $R = R_p$  and  $R = 0.5$  under SNR=21.6dB, Solid line corresponds to  $R = R_p$  while dashed line corresponds to  $R = 0.5$

sensitivity penalty varying with the decay parameter  $k$  when obtaining a BER of  $10^{-9}$ . The solid line represents the curve when  $R$  is set at the optimal value  $R_p$  while the dashed line is set at 0.5, respectively. Obviously, the sensitivity penalty is reduced by optimizing the detection threshold. When  $k = 0.05$  and  $k = 0.10$ , a 0.8dB and 2.8dB penalty can be reduced respectively.

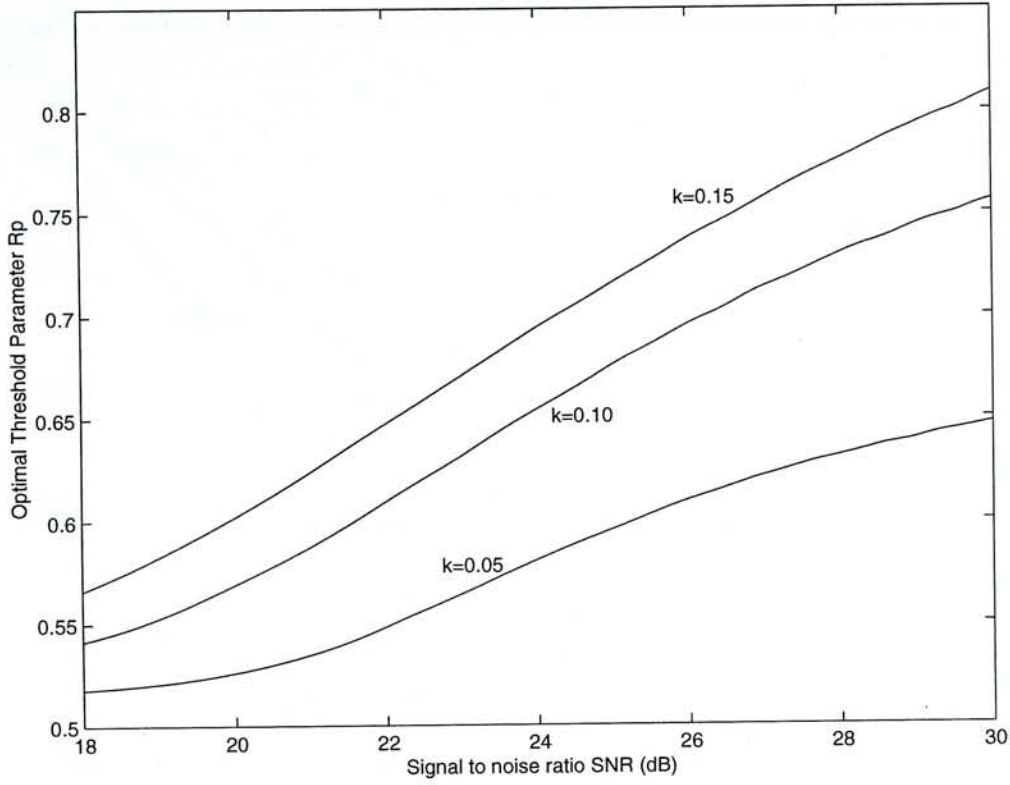


Figure 3.5: Optimal threshold parameter  $R_p$  versus SNR at  $k = 0.05$ ,  $k = 0.10$  and  $k = 0.15$

### 3.5 Simulation Result on the BER of Burst-mode Receiver

We have theoretically analyzed the BER performance of the burst-mode receiver and proposed a way to set an optimal detection threshold to get the best BER performance. To verify the theoretical model, computer simulations of burst-mode receiver are performed.

Our simulation model is shown in Fig.3.8. A uniform distributed pseudo-random binary sequence  $N = 2^{15} - 1$  is first generated. The sequence then goes directly to a transmission channel where Gaussian distributed noise is added. The noise added binary sequence then reaches the detector. The detection



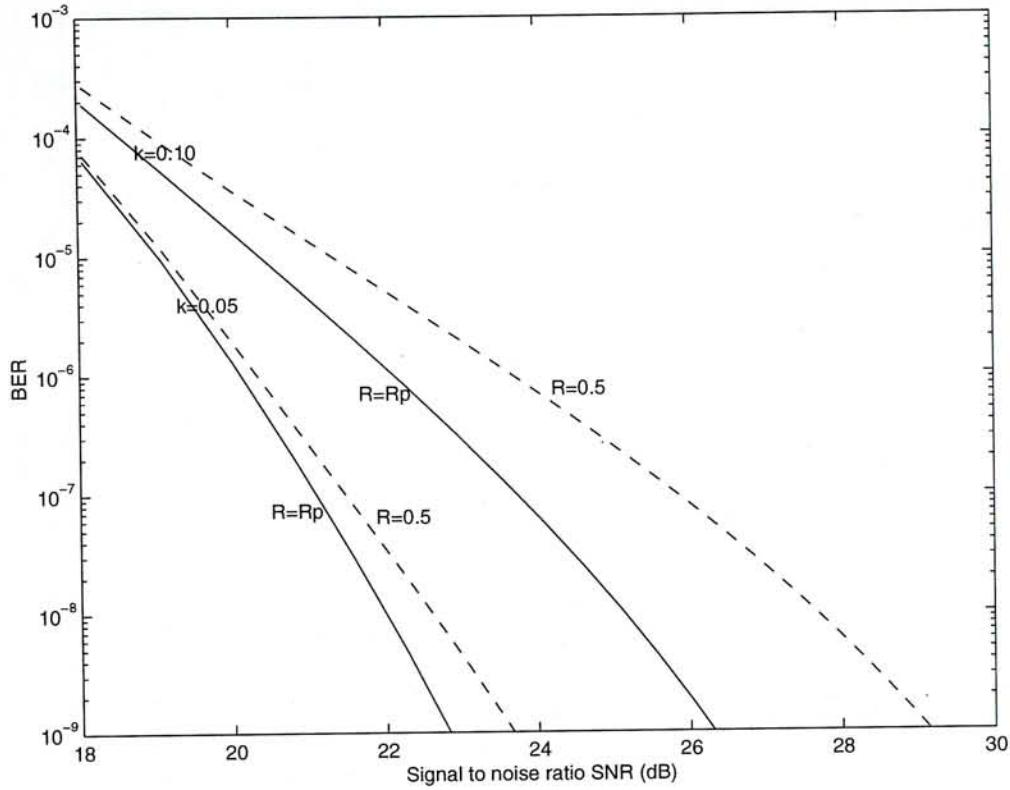


Figure 3.6: Bit error rate versus SNR at  $k = 0.05$  and  $k = 0.10$ . Solid lines are the optimized BER, dashed lines are the BER when  $R = 0.5$

threshold is preset at the optimal value according to our previous calculation. The instantaneous decision threshold for determining each incoming signal conforms to the Markov relationship by equation (3.1). The output of the detector is the recovered data with errors. By comparing the output sequence with the original input, we can obtain the BER of the receiver. When we change the value of  $k$ , the BER with respect to different  $k$  values can be obtained.

The relationship between the decay parameter  $k$  and the BER under  $SNR = 21.6dB$  is shown in Fig.3.9. For comparison, we put the previous theoretical result together with the simulation result, we can see that they agree with one another very well.

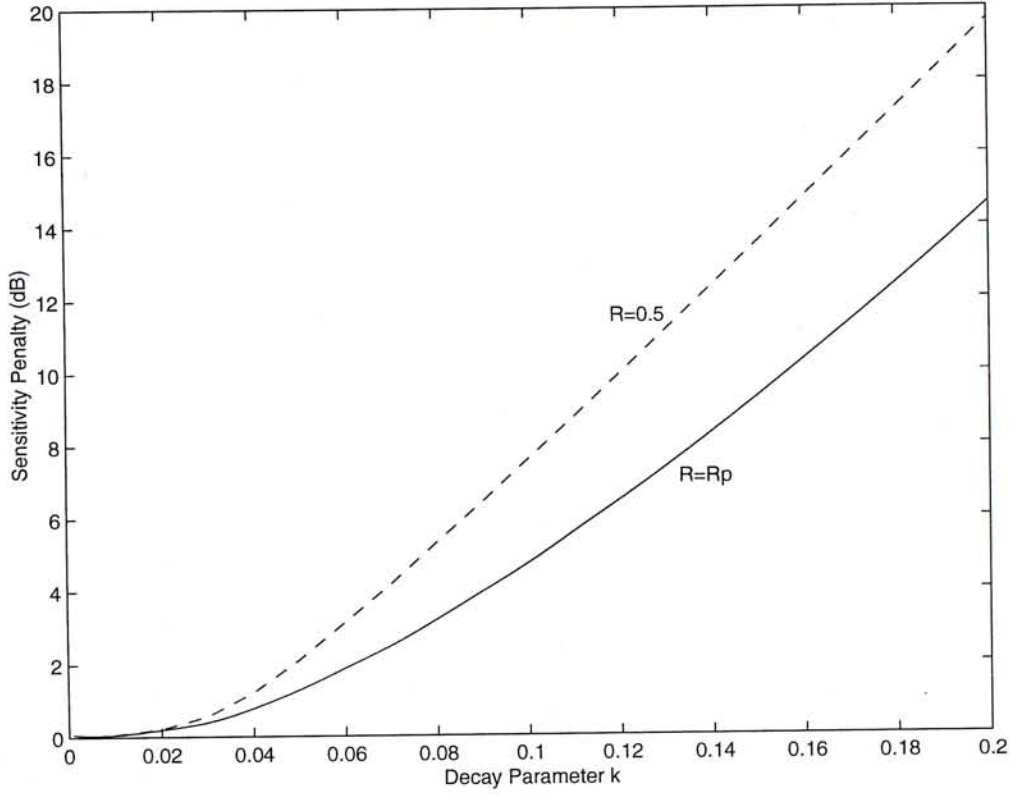


Figure 3.7: Sensitivity penalty versus the decay parameter  $k$

### 3.6 Chapter Summary

In this chapter we have investigated the threshold fluctuation and the BER performance of burst-mode receivers. As the adaptive threshold control circuit of the burst-mode receiver employs a natural charge/discharge mechanism, the preset threshold will decay with the signal while receiving data. The analyze this decay process suggested that it is more appropriate to preset the detection threshold at an optimal value instead of the midway between level of symbol “1” and “0”. Numerical calculation and simulation indicated that the BER will be improved by doing so. Accordingly, the sensitivity penalty with respect to continuous-mode receiver can be reduced.

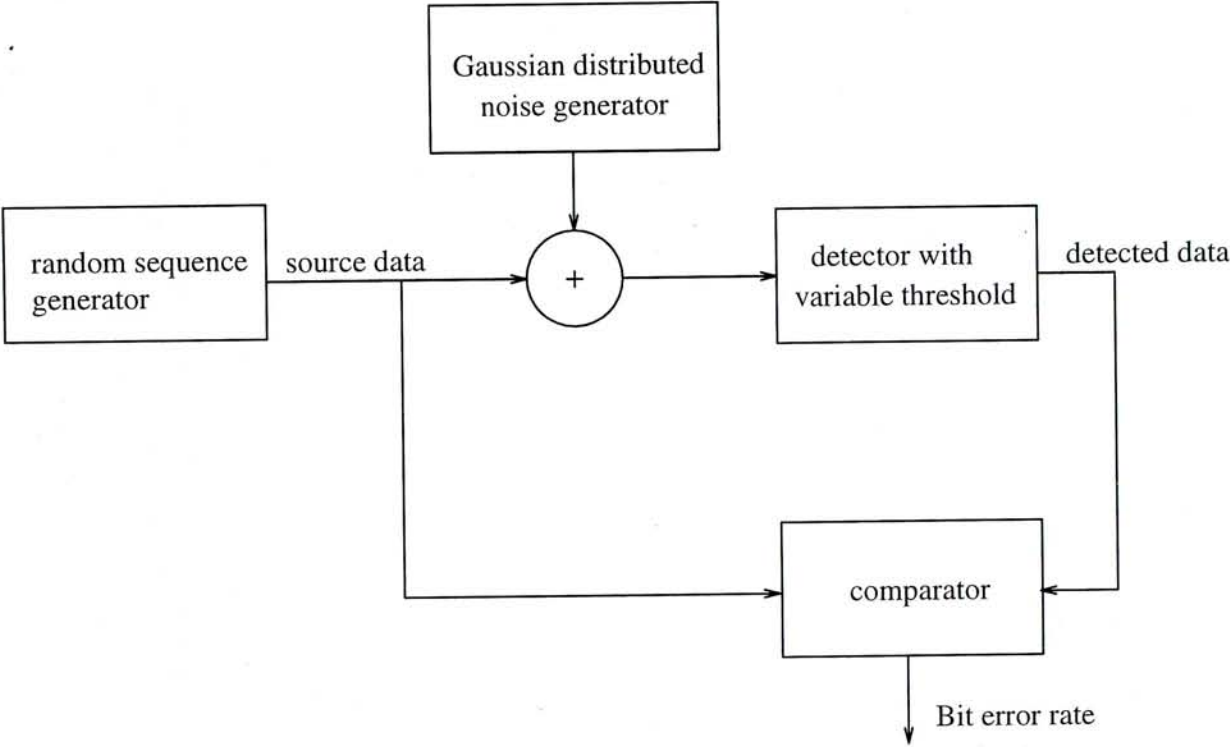


Figure 3.8: Simulation diagram of BER performance for burst-mode receiver



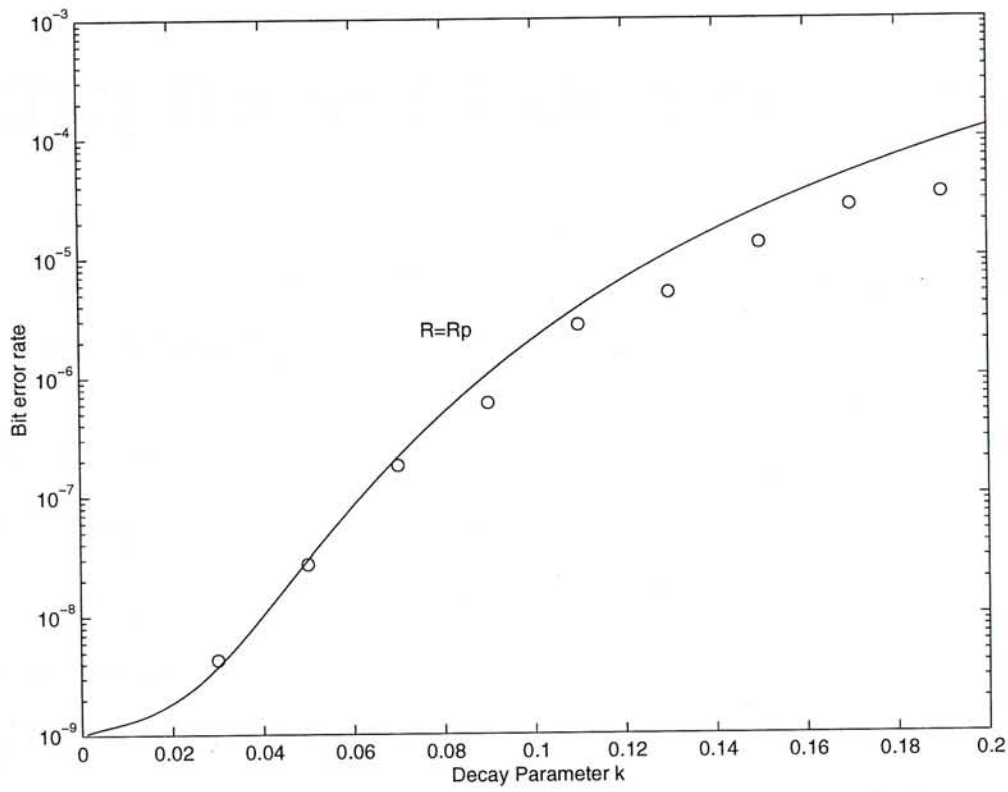


Figure 3.9: Simulation results of BER versus decay parameter when  $SNR = 21.6dB$ . Little circles represent the simulation results, solid line represents the theoretical result.

# Chapter 4

## MLT-3 Burst-Mode Receiver

### 4.1 Introduction

Fiber Distributed Data Interface (FDDI) is a 100 Mbps fiber optic local area network (LAN) standard being developed by American National Standard Institute. It is widely accepted and supported in the industry for high-speed multivendor networking. As the cost of installing fibers is more expensive than the existing copper wiring, the FDDI standard is currently being extended to run over high-quality copper cables, which is known as CDDI under such situations [24, 25].

The high-frequency signals over copper wires cause the problem of electromagnetic interference (EMI). After 4B/5B encoding, the FDDI signal has a bit rate of 125 Mbps. With NRZI encoding the signal frequency is of 62.5 MHz. At this frequency range, the copper wire acts as a broadcasting antenna. The electromagnetic radiations from the wire interfere with radio and television transmissions. The interference increases with the signal level. Strict limits on such

EMI are laid down in many countries.

One solution to the EMI problem is to use shielded twisted-pair (STP), which has a special metallic shield surrounding to prevents interference. Another solution is to use special coding techniques that result in a lower frequency signal. The advantage of this second approach is that the unshielded twisted-pair (UTP), which reach all desks, can be used for FDDI.

A well-known method to reduce the frequency spectrum is to increase the number of amplitude levels in signal, that is, to use multilevel coding. A three-level coding techniques called multilevel transmission 3 (MLT-3) has been selected to run FDDI over UTP [26]. This reduces the signal frequency by a factor of 2.

Since the copper-based multiaccess local area networks are very cost-effective, currently there is great demand in transmitting high speed signal over UTP wires. Therefore it is desirable to develop MLT-3 burst-mode receivers for this kind of networks [27]. In this chapter, we will first introduce the MLT-3 line code and investigate the BER performance of MLT-3 continuous-mode receiver. Then we will propose a schematic of feed-forward burst-mode receiver for MLT-3 data reception and show how the threshold decay affects the performance in burst-mode receiver. Finally we utilize the optimal threshold to optimize the BER.

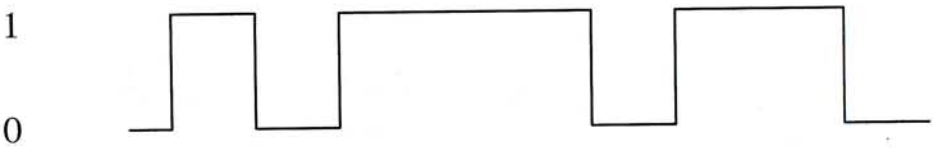
## **4.2 MLT-3 Line Code**

MLT-3 is a three-level coding chosen to reduce the frequency spectrum in high-speed data transmission. It is basically an extension of NRZI to three levels, so

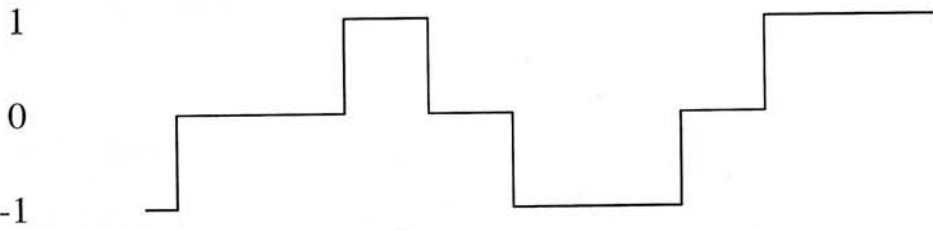




it is often called NRZI-3. The three levels are denoted by +1, 0, and -1. Like NRZI, a “zero” bit is coded as the absence of a transition and a “one” bit is coded as a transition. The successive transitions are all in the same direction (ascending or descending) except when the signal reaches a level of +1 or -1, at which point the direction is reversed. Fig.4.1 shows a sample NRZ code-bit string and the corresponding MLT-3 coding signal.



(1) Binary NRZ code {1 0 1 1 1 0 1 1 0}



(2) MLT-3 line code {0 0 +1 0 -1 -1 0 +1 +1}

Figure 4.1: MLT-3 coding of sample stream

The complete transition diagram is shown in Fig.4.2. It consists of four states labeled as +1, 0<sup>+</sup>, 0<sup>-</sup>, and -1. The labels indicate the level of the signal when the system is in that state. The input bits are represented by arcs. Thus, if the signal level is +1 and a zero is to be sent, the signal level remains +1 in the next

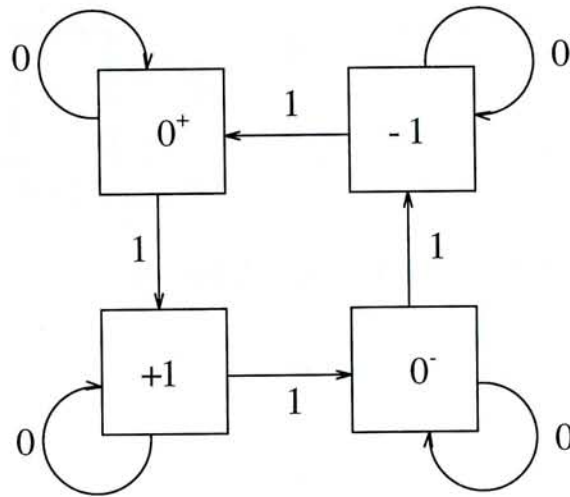
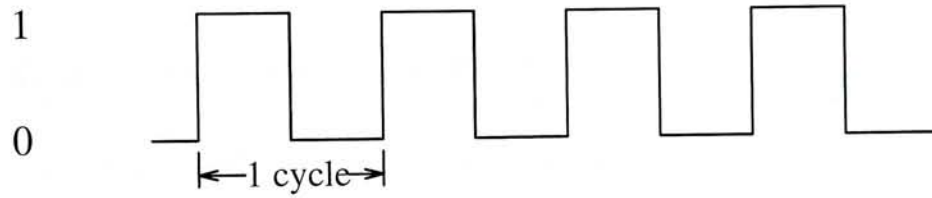


Figure 4.2: MLT-3 transition state diagram

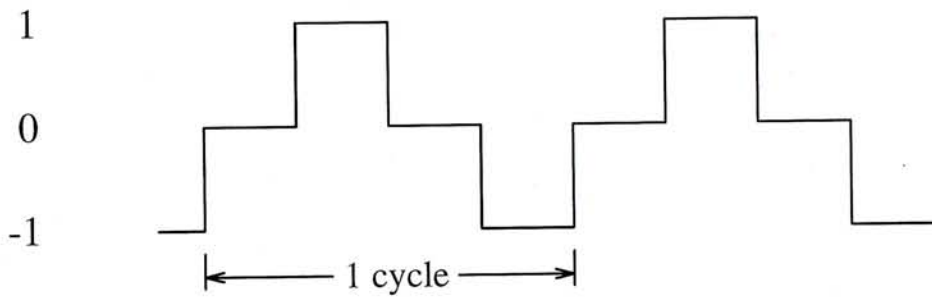
bit period. On the other hand, if a one is to be sent, the signal level is changed to 0 (state  $0^-$ ). Another one in this state will cause the signal level to change to -1.

To see the effect of multilevel encoding on the signal frequency, consider the NRZI and MLT-3 encodings of a stream of "1"s. The signals for these two encodings are shown in Fig.4.3. It is shown that each cycle of the signal consists of two bit times with NRZI but four bit times with MLT-3. Assuming an FDDI bit rate of 125 Mbps, the binary NRZI signal has a frequency of 62.5 MHz while the frequency for MLT-3 is 31.25 MHz.





(1) Binary NRZI code {1 0 1 0 1 0 1 0}



(2) MLT-3 code {0 +1 0 -1 0 +1 0 -1}

Figure 4.3: NRZI and MLT-3 coding a stream of "1"s

### 4.3 BER Performance of MLT-3 Continuous-Mode Receiver

The error performance of MLT-3 line code reception can be found by extending the case of binary reception. We still assume the additive noise to be Gaussian distributed.

Let  $P(+1)$ ,  $P(0)$  and  $P(-1)$  be the probability of +1, 0 and -1 transmitted by the MLT-3 encoder at the source, where  $P(+1) + P(0) + P(-1) = 1$ . Let  $P(e/+1)$ ,  $P(e/0)$  and  $P(e/-1)$  be the individual probability of error occurring

when +1, 0 and -1 are received. The total probability of error may then be expressed as

$$BER = P(e/+1)P(+1) + P(e/0)P(0) + P(e/-1)P(-1). \quad (4.1)$$

The voltages for signal +1 and -1 have the same absolute value but antipolar, thus we assume  $V_{+1} = -V_{-1} = V_1$ . The voltage for signal 0 is zero, i.e.,  $V_0 = 0$ . At the receiver side, the three signal voltage levels are observed to be

$$\begin{aligned} y_{+1} &= V_1 + n \\ y_0 &= 0 + n \\ y_{-1} &= -V_1 + n \end{aligned} \quad (4.2)$$

where  $n$  represents the additive noise. If  $n$  is Gaussian distributed with zero

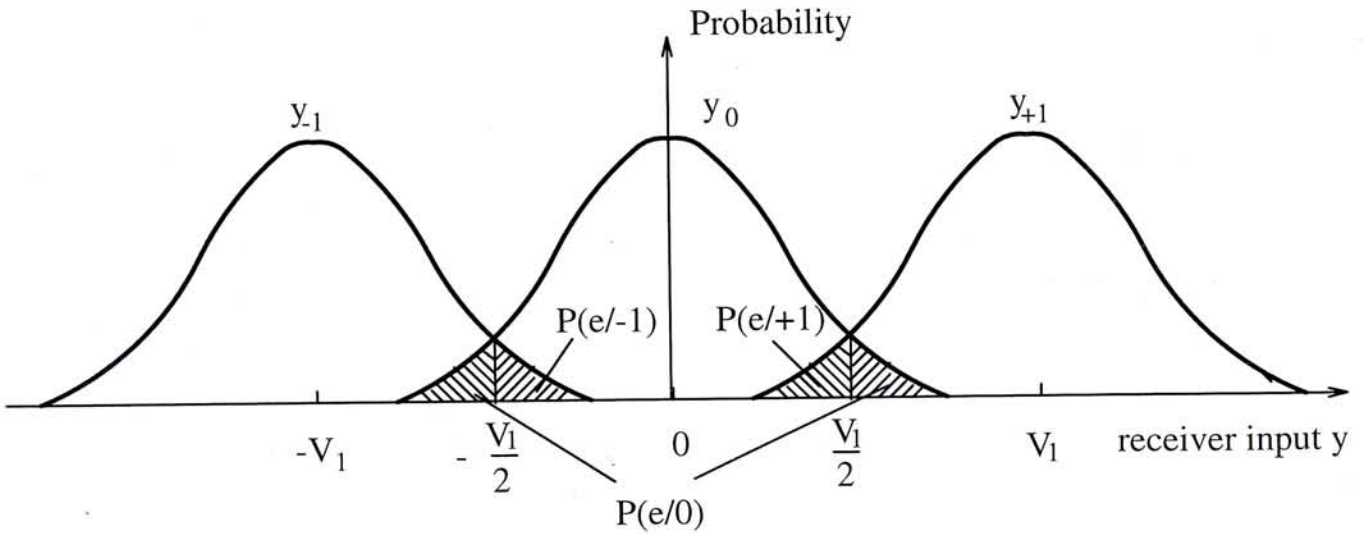


Figure 4.4: Probability density functions for MLT-3 transmission over additive Gaussian noise channel

mean and variance  $\sigma^2$ , it follows that  $y_{+1}$ ,  $y_0$  and  $y_{-1}$  are all Gaussian distributed

with variance  $\sigma^2$  but with mean  $\bar{y}_{+1} = V_1$ ,  $\bar{y}_0 = 0$  and  $\bar{y}_{-1} = -V_1$  respectively. Fig.4.4 shows their probability density functions.

In continuous data reception, to achieve the minimum BER, the decision thresholds must be placed at halfway between signal levels, that is, at  $-V_1/2$  and  $V_1/2$ . The receiver would determine the signal as +1 if  $y > V_1/2$ , as -1 if  $y < -V_1/2$ , and as 0 if  $-V_1/2 < y < V_1/2$ .

The error probabilities  $P(e/+1)$ ,  $P(e/0)$  and  $P(e/-1)$  are simply the shaded areas under the curves in Fig.4.4. In equation form these probabilities are

$$\begin{aligned}
 P(e/+1) &= \frac{1}{\sigma\sqrt{2\pi}} \int_{-\infty}^{V_1/2} \exp\left[-\frac{(V - V_1)^2}{2\sigma^2}\right] dV \\
 &= \operatorname{erfc}\left(\frac{V_1}{2\sigma}\right) \\
 P(e/0) &= \frac{1}{\sigma\sqrt{2\pi}} \left\{ \int_{-\infty}^{-V_1/2} \exp\left[-\frac{V^2}{2\sigma^2}\right] dV + \int_{V_1/2}^{\infty} \exp\left[-\frac{V^2}{2\sigma^2}\right] dV \right\} \\
 &= 2\operatorname{erfc}\left(\frac{V_1}{2\sigma}\right) \\
 P(e/-1) &= \frac{1}{\sigma\sqrt{2\pi}} \int_{-V_1/2}^{\infty} \exp\left[-\frac{(V + V_1)^2}{2\sigma^2}\right] dV \\
 &= \operatorname{erfc}\left(\frac{V_1}{2\sigma}\right)
 \end{aligned} \tag{4.3}$$

where  $\operatorname{erfc}(x)$  is the complementary error function.

It can be seen from Fig.4.2 that MLT-3 code has four states and each state occurs equally. Since the two states  $0^+$  and  $0^-$  have the same signal level 0, it is easy to know that the probability of +1, 0 and -1 being transmitted are

$P(+1) = \frac{1}{4}$ ,  $P(0) = \frac{1}{2}$ ,  $P(-1) = \frac{1}{4}$ . Thus equation (4.1) results in

$$\begin{aligned} BER &= \frac{1}{4}P(e/+1) + \frac{1}{2}P(e/0) + \frac{1}{4}P(e/-1) \\ &= \frac{3}{2}erfc\left(\frac{V_1}{2\sigma}\right). \end{aligned} \quad (4.4)$$

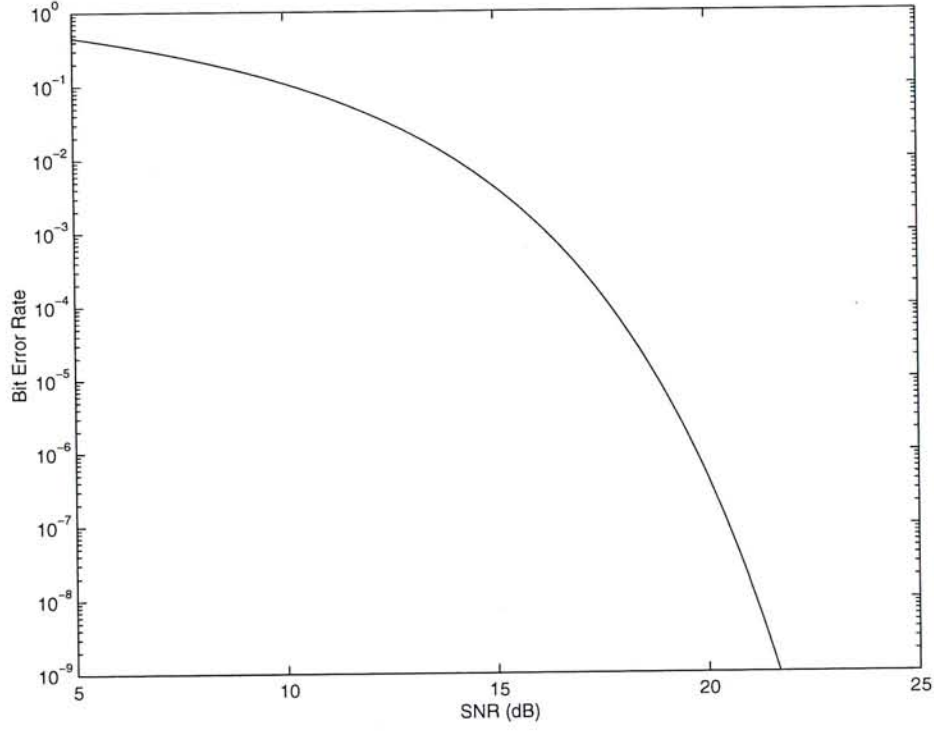


Figure 4.5: BER versus SNR in MLT-3 code

These results can be related to signal-to-noise ratio SNR by noting that

$$SNR = \frac{V_1^2}{\sigma^2}. \quad (4.5)$$

Hence equation (4.4) can be rewritten as

$$BER = \frac{3}{2}erfc(\sqrt{SNR}/2). \quad (4.6)$$

When approximated by  $erfc(x) = \frac{1}{x\sqrt{2\pi}}e^{-x^2/2}$ ,

$$BER = \frac{3}{\sqrt{2\pi SNR}}e^{-SNR/8}. \quad (4.7)$$



Fig.4.5 gives the relationship between the BER and SNR in MLT-3 code continuous-mode receiver. In order to get a BER no less than  $10^{-9}$ , SNR has to be at least 21.8dB.

## 4.4 Burst-mode Receiver For MLT-3 Line Code

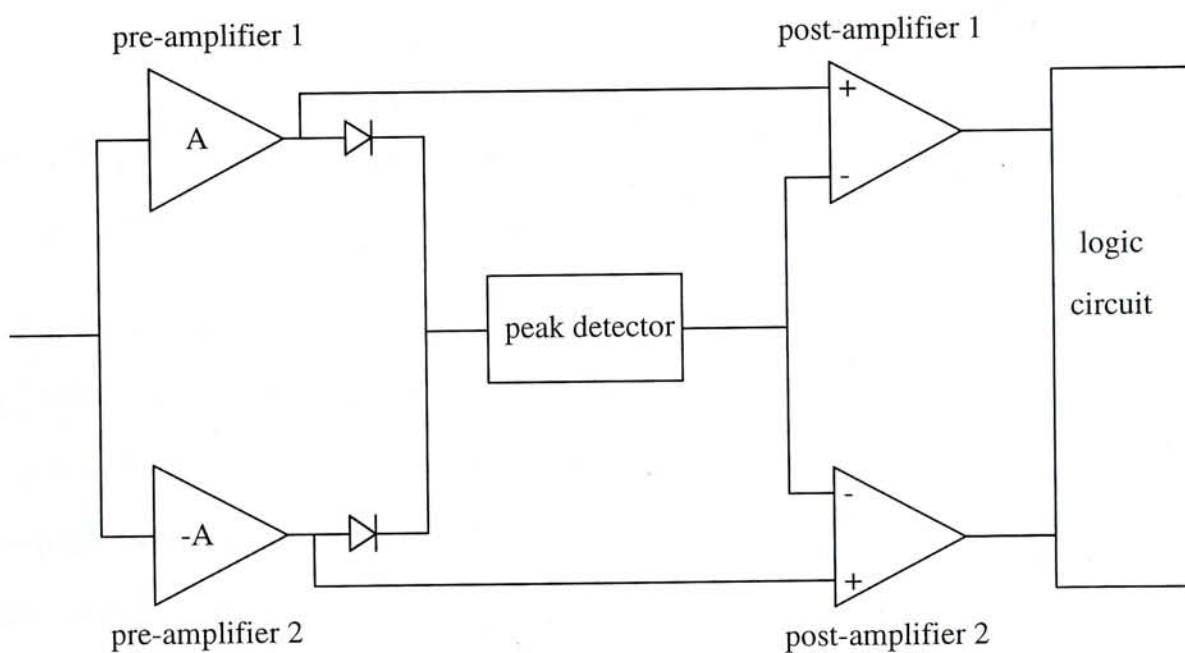


Figure 4.6: Schematic diagram of MLT-3 burst-mode receiver

A block diagram of a receiver suitable for MLT-3 burst-mode signal reception can be designed as shown in Fig.4.6. It is DC-coupled to adapt to the bursty data, with two signal branches and a feed-forward structure.

The preamplifier in the upper branch has a positive gain while the one in the lower branch has a negative gain of the same value. Due to the presence of

the two diodes, an input signal “+1” will charge the capacitor in peak detector through the upper branch, whereas an input “-1” will charge it through the lower branch. The peak detector detects the threshold and provides it to the two post-amplifiers. The signal is discriminated at the post-amplifiers as follows:

- when the input signal is “+1”, post-amplifier 1 will give a positive output and post-amplifier 2 will give a negative output;
- when the input signal is “-1”, post-amplifier 2 will give a positive output and post-amplifier 1 will give a negative output;
- when the input signal is “0”, both post-amplifier 1 and 2 will give negative outputs.

Theoretically there should be two detection thresholds for reception of three-level MLT-3 signal. But as they have the same value with opposite polarity, only one peak detector is used at the receiver to detect their absolute value. This threshold value is data pattern dependent just like the threshold fluctuation in binary burst-mode receiver.

The variation of the two thresholds is shown in Fig.4.7. At the beginning of each MLT-3 burst-mode packet, a preamble field consisting of bit “+1”s presets the detection threshold. Then, in the signal field, when the incoming data is “+1” or “-1”, the threshold will be charged up to the preset threshold very quickly; when the incoming signal is “0”, the threshold will be discharged and decay.

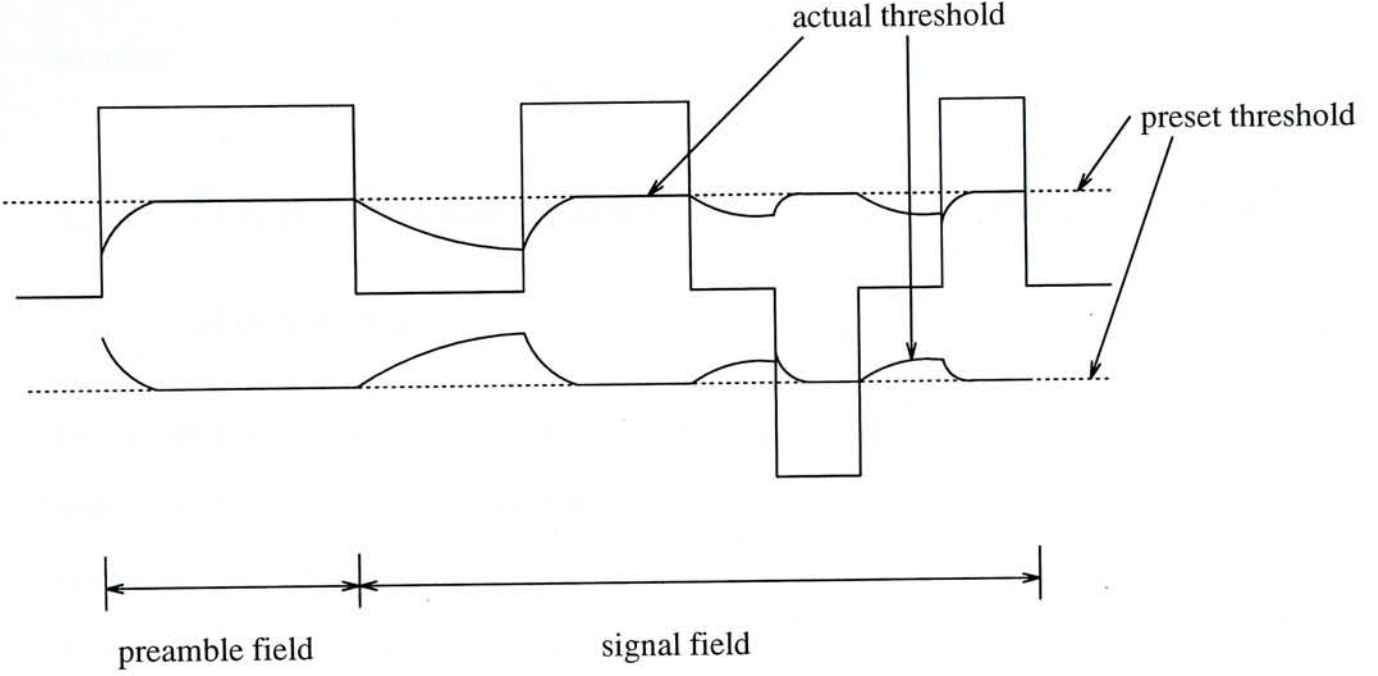


Figure 4.7: Threshold variation of MLT-3 burst-mode receiver

We denote the preset detection threshold as  $V_T$ , the actual fluctuating threshold can be given by

$$V[m, t] = \begin{cases} V[m-1, T]e^{(-t/\tau_f)} & a(m) = "0" \\ V[m-1, T] + (V_T - V[m-1, T])(1 - e^{-t/\tau_r}) & a(m) = "+1" \text{ or } "-1" \end{cases} \quad (4.8)$$

where the variables have the same meaning as in equation (3.1).

As the charging time (rising time) constant  $\tau_r$  is set quite small, the instantaneous detection threshold for bit "+1" or "-1" can approximately approach  $V_T$ , that is,  $V_{T1} = V_T$ . In a stream of consecutive "0"s, the instantaneous threshold for the  $j$ th "0" can be obtained as in a binary burst-mode receiver, given by

$$V_{T0j} = V_T e^{-(j-1/2)k}, \quad (4.9)$$

where  $k = T/\tau_f$  is defined as the decay parameter, and bit detection instant is assumed to be at the center of the bit period which has the maximum eye opening.

## 4.5 BER Performance of MLT-3 Burst-Mode Receiver

For a MLT-3 signal sequence encoded from a pseudo-random binary sequence with length  $N = 2^n - 1$ , the probability of  $i$  consecutive "0"s present in the string is still  $1/2^{i+1}$ . The error probability for the  $j$ th "0" is denoted by  $P(e/0)_j$ . Then in MLT-3 burst-mode receiver the BER expression of equation (4.1) can be rewritten as

$$BER = \frac{1}{4}P(e/+1) + \sum_{i=1}^n \frac{1}{2^{i+1}} \frac{1}{i} \sum_{j=1}^i P(e/0)_j + \frac{1}{4}P(e/-1). \quad (4.10)$$

where

$$\begin{aligned} P(e/+1) &= \frac{1}{\sigma\sqrt{2\pi}} \int_{-\infty}^{V_{T1}} \exp\left(-\frac{(V - V_1)^2}{2\sigma^2}\right) dV \\ &= \operatorname{erfc}\left(\frac{V_1 - V_{T1}}{\sigma}\right) \\ P(e/0)_j &= \frac{1}{\sigma\sqrt{2\pi}} \left( \int_{-\infty}^{-V_{T0j}} + \int_{V_{T0j}}^{\infty} \right) \exp\left(-\frac{V^2}{2\sigma^2}\right) dV \\ &= 2\operatorname{erfc}\left(\frac{V_{T0j}}{\sigma}\right) \end{aligned}$$



$$\begin{aligned}
 P(e/ - 1) &= \frac{1}{\sigma\sqrt{2\pi}} \int_{-V_{T1}}^{\infty} \exp\left(-\frac{(V + V_1)^2}{2\sigma^2}\right) dV \\
 &= \operatorname{erfc}\left(\frac{V_1 - V_{T1}}{\sigma}\right).
 \end{aligned} \tag{4.11}$$

If we define

$$\begin{aligned}
 Q_1 &= \frac{V_1 - V_{T1}}{\sigma} \\
 Q_{0j} &= \frac{V_{T0j}}{\sigma}
 \end{aligned} \tag{4.12}$$

equation (4.10) can be rewritten as

$$\begin{aligned}
 BER &= \frac{1}{2} \operatorname{erfc}(Q_1) + 2 \sum_{i=1}^n \frac{1}{2^{i+1}} \frac{1}{i} \sum_{j=1}^i \operatorname{erfc}(Q_{0j}) \\
 &\approx \frac{1}{2} \frac{\exp(-Q_1^2/2)}{\sqrt{2\pi}Q_1} + 2 \sum_{i=1}^n \frac{1}{2^{i+1}} \frac{1}{i} \sum_{j=1}^i \frac{\exp(-Q_{0j}^2/2)}{\sqrt{2\pi}Q_{0j}}.
 \end{aligned} \tag{4.13}$$

To obtain the minimum BER, the thresholds should not be centered halfway between the signal levels any more. We can use the same method as we used in the binary code burst-mode receiver to get the optimal detection threshold for MLT-3 burst-mode receiver.

$R$  is the threshold parameter used to describe the position of threshold setting, defined as

$$R = \frac{V_T}{V_1}. \tag{4.14}$$

We can find the optimal threshold parameter  $R_p$  from

$$\frac{d(BER)}{dR} = 0. \tag{4.15}$$

Utilizing equation (4.9), (4.12), (4.13) and (4.14),  $R_p$  can be obtained by means of numerical calculation.

$R_p$  depends on both the decay parameter  $k$  and the signal SNR. Here  $SNR = V_{+1}^2/\sigma^2$ . Fig.4.8 and Fig.4.9 shows  $R_p$  as a function of  $k$  and SNR, respectively. When  $k$  or SNR becomes larger,  $R_p$  will increase accordingly.

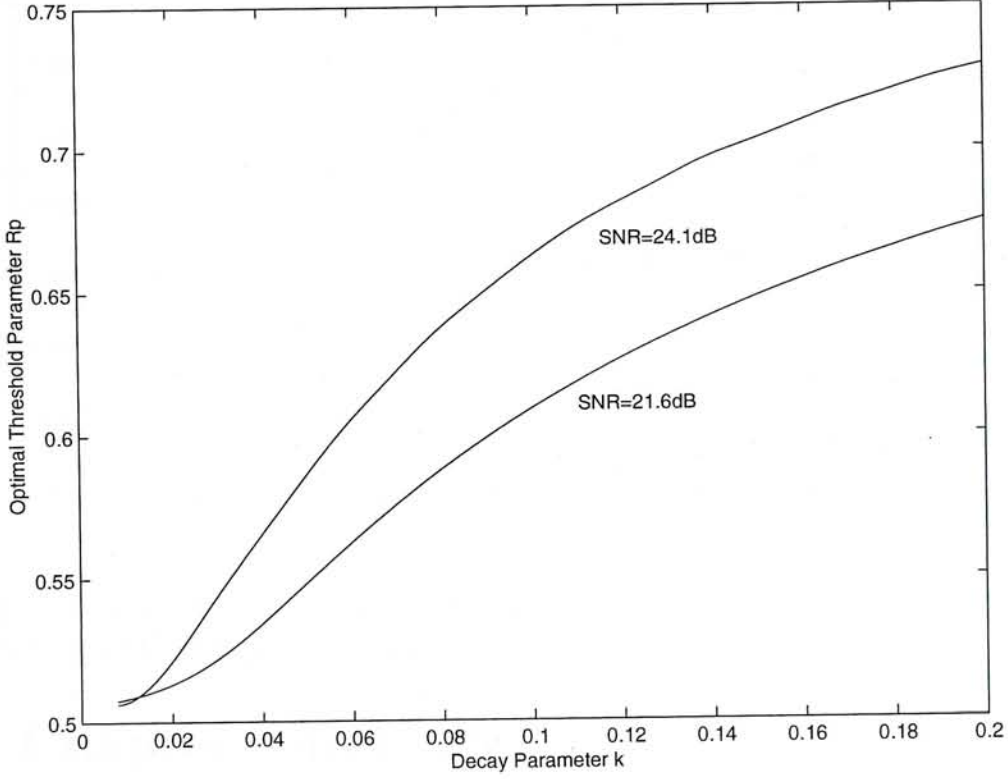


Figure 4.8: Optimal threshold parameter  $R_p$  versus the decay parameter  $k$  under SNR=21.6dB and SNR=24.1dB in MLT-3 burst-mode receiver

Fig.4.10 is the BER versus the decay parameter when the detection threshold is optimized under  $SNR = 21.6dB$ . Fig.4.11 shows the relationship between BER and SNR. Solid line represents the condition at  $k = 0.05$ , while dashed line represents BER of continuous-mode MLT-3 receiver. It is easy to notice that a larger SNR is needed to get the same BER performance in burst-mode receiver than the continuous one. Fig.4.12 shows the sensitivity penalty as a function of  $k$  for maintaining a BER of  $10^{-9}$  in MLT-3 burst- mode receiver.

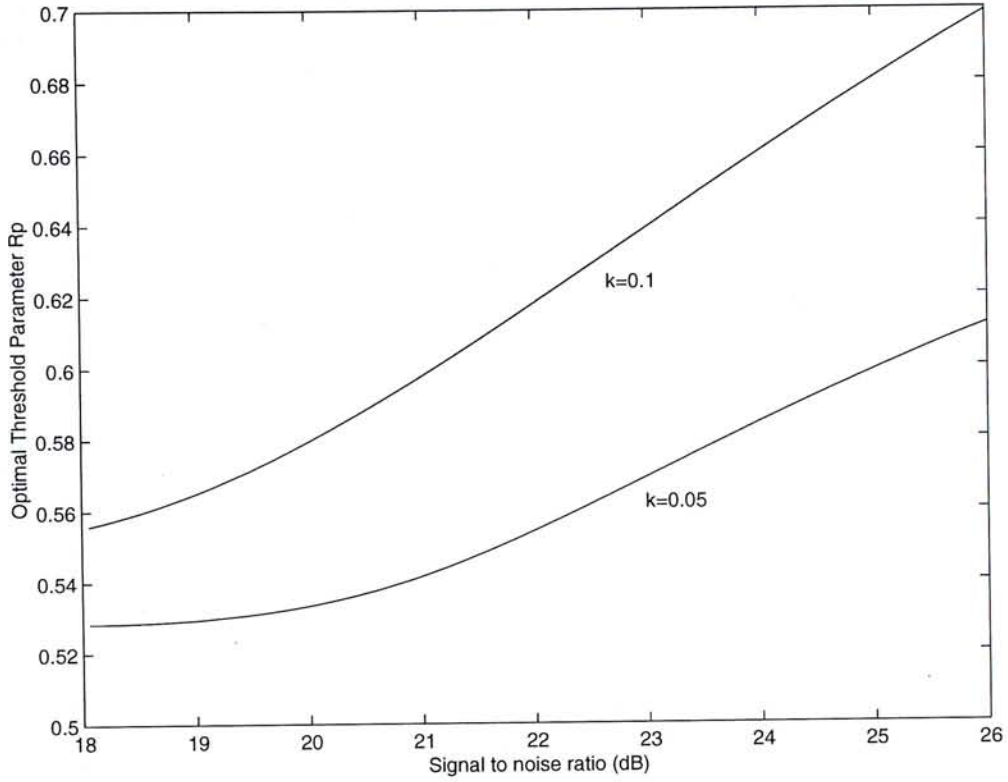


Figure 4.9: Optimal threshold parameter  $R_p$  versus the signal SNR at  $k=0.05$  and  $k=0.10$  in MLT-3 burst-mode receiver

## 4.6 Chapter Summary

In this chapter we have designed a receiver for MLT-3 burst-mode code signals. BER performances of both the continuous-mode receiver and burst-mode receiver have been evaluated. MLT-3 Burst-mode receiver has a BER degradation because of the decay characteristics of the adaptive threshold control circuit (peak detector). Similar to the binary burst-mode receiver, the detection threshold can be set at the optimal position to get the best performance.

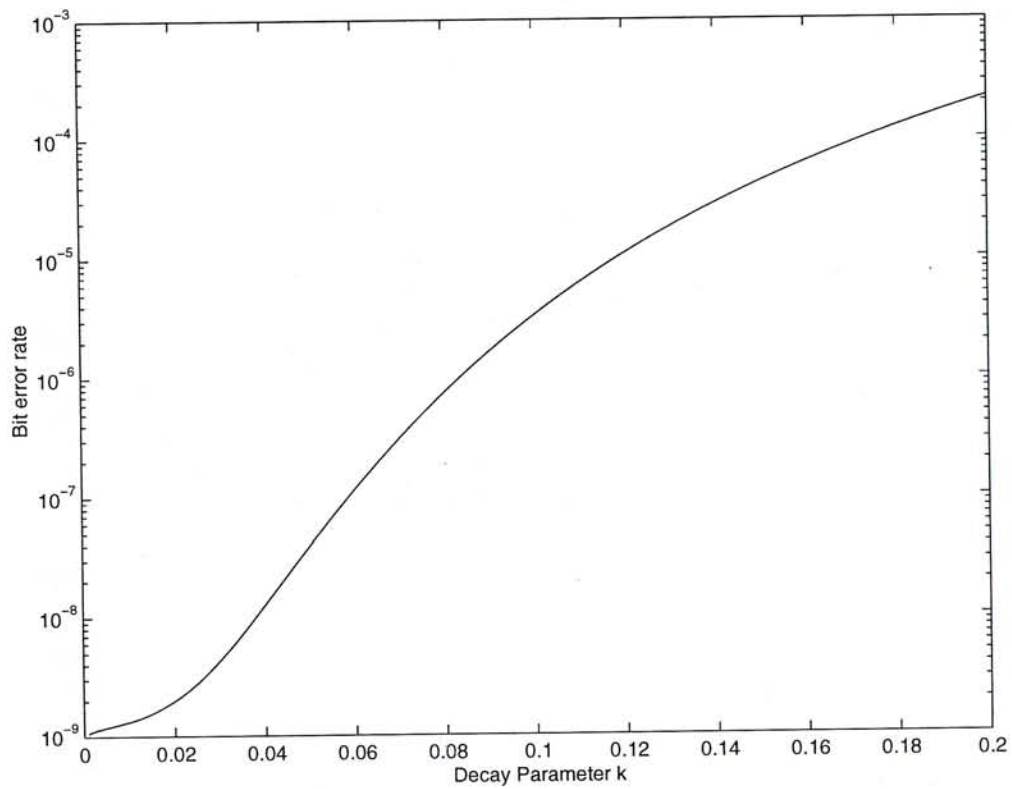


Figure 4.10: BER versus the decay parameter  $k$  when  $R = R_p$  under SNR=21.6dB in MLT-3 burst-mode receiver



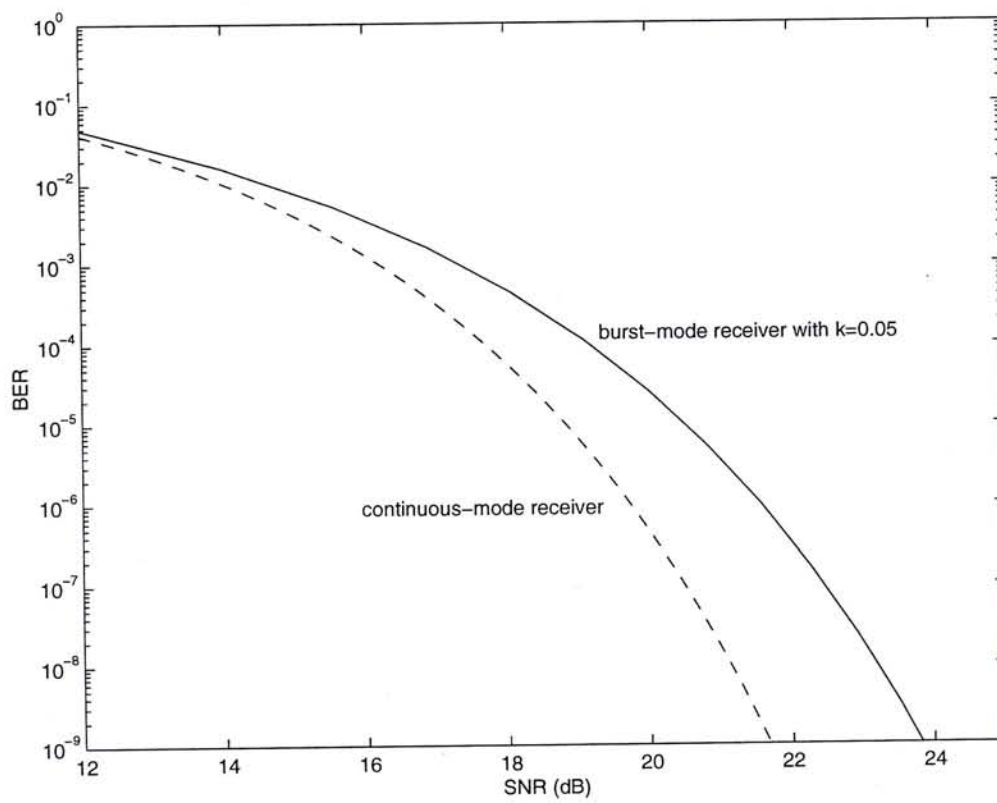


Figure 4.11: BER versus SNR when  $k = 0.05$  and  $k = 0$  in MLT-3 burst-mode receiver

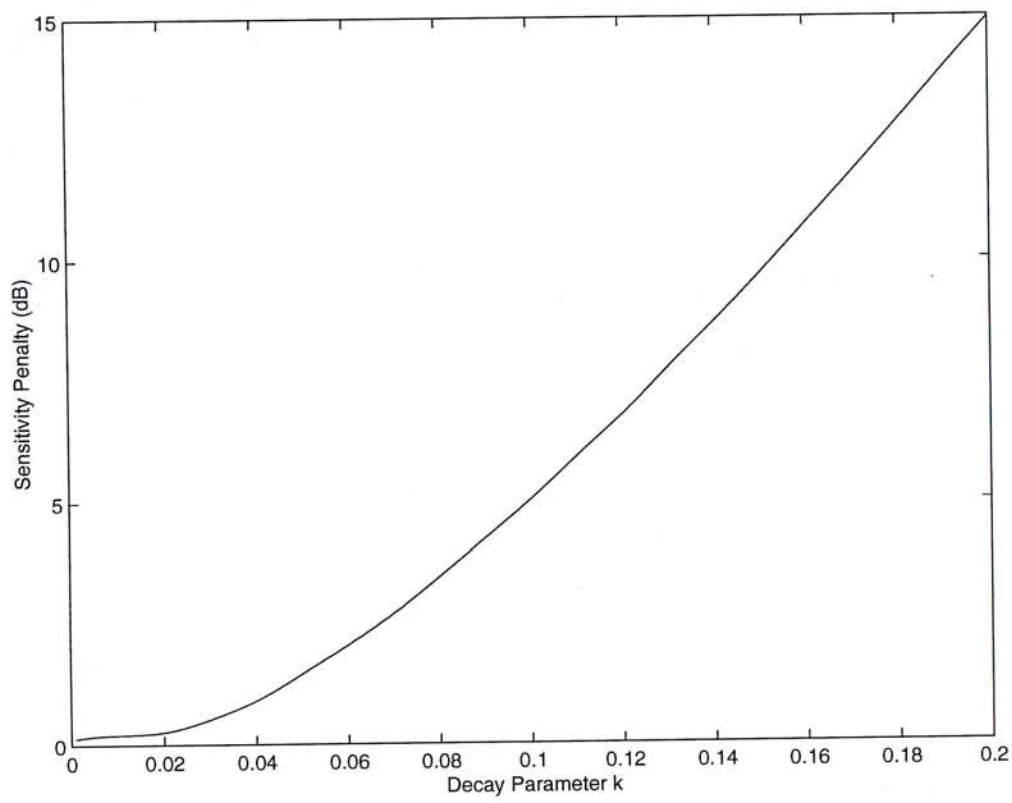


Figure 4.12: Sensitivity penalty versus k to maintain a BER of  $10^{-9}$  in MLT-3 burst-mode receiver

# Chapter 5

## Conclusion

The thesis investigated the performance of existing binary burst-mode receiver and proposed to choose an optimal detection threshold to improve the BER. In addition, a schematic of multi-level MLT-3 burst-mode receiver was described and its BER performance was evaluated.

Optical burst-mode receivers are having more and more applications in multi-access networks, access loops and intercomputer communications. For instance, burst-mode compatible receivers are required in optical bus applications for high-speed transmission, because of their capability in handling closely spaced packet signal with varying optical power. Another example is burst-mode packet transmission in numerous point-to-multipoint communication systems including passive optical networks (PON's) for digital telephony, local area and metropolitan networks. These systems are based on passive optical networks in either a star or bus configuration and TDMA multiplexing is typically used for transmission from the subscriber to the central office. In this multiplexing scheme the remote subscribers transmit data to the central office in designated time slots, resulting





in bursts of signals which have varying amplitude level and uncertain phase. Burst-mode receivers are required in the central office to receive these burst and packet mode data.

To design a digital burst-mode receiver, fast amplitude recovery and phase recovery should be taken into considerations. As far as amplitude recovery is concerned, an adaptive threshold control circuit should be designed in such a way that it can dynamically detect the amplitude of the bursty packets. Currently the common method is to employ a DC-coupled receiver, instead of the conventional AC-coupled one, to meet the variable amplitude range. A preamble field of several bit "1"s is attached at the beginning of each incoming packet to determine threshold.

In this thesis special attention was devoted to appropriately setting the threshold position between the signal symbols. Currently the detection threshold in binary burst-mode receiver is usually set at the midway between amplitude of bit "1" and bit "0", same as in continuous-mode receiver with a fixed detection threshold. However, the BER performance is not optimized under this setting. As illustrated in the performance evaluation theory proposed by Su et al., the preset detection threshold will decay while receiving bit "0"s because of the characteristic of the adaptive threshold control circuit. Thus based on the BER evaluation of the threshold decay factor, we found the optimal detection threshold by numerical computation. Comparison of burst-mode receiver performance using the midlevel and the optimal threshold settings was presented. The results indicate that better BER performance can be achieved choosing an optimal threshold. To verify the theoretical results, a computer simulation on the performance of burst-mode receiver was performed and the simulation

results agree well with the theoretical ones.

A three-level coding MLT-3, which is standardized for transmission of high-speed data over UTP cables, can be used in burst-mode data transmission. We proposed a schematic for MLT-3 burst-mode receiver. BER performance of burst-mode MLT-3 receivers was evaluated and compared with that of the continuous-mode receivers. BER degradation and SNR penalty were observed in the burst-mode receiver due to the threshold decay effect in the adaptive threshold control circuit. To obtain the best BER performance, optimal detection threshold was determined by numerical calculation.

# Bibliography

- [1] S. Shimada et al., "Very High-Speed Optical Signal Processing," *Proc. IEEE*, vol. 81, no. 11, pp. 1633-1646, Nov. 1993.
- [2] O. Gerstel, "On the future of wavelength routing networks," *IEEE Network*, vol. 10, no. 9, pp. 32-36, Nov/Dec. 1996.
- [3] N. K. Cheung et al., "Dense Wavelength Multiplexing for High Capacity and Multiple Access Communications Systems," *IEEE J. Selected Areas of Communication*, Vol. JSAC-8, No. 6, pp. 945-947, Aug. 1990.
- [4] J. R. Stern et al., "Passive optical local networks for telephony applications and beyond," *Electron. Lett.*, vol. 23, pp. 1255-1257, 1987.
- [5] Y. M. Lin et al., "Passive optical subscriber loops with multiaccess," *IEEE J. Lightwave Tech.*, vol. 7, pp. 1769-1777, 1989.
- [6] I. M. McGregor et al., "Implementation of a TDM optical network for subscriber loop applications," *IEEE J. Lightwave Tech.* vol. LT-7, no. 11, pp. 1752-1758, Nov. 1989.
- [7] J. W. Ballance et al., "ATM access through a passive optical network," *Electron. Lett.*, vol. 26, no. 9, pp. 558-560, Apr. 1990.



- [8] T. R. Rowbotham et al., "Local loop development in the U. K.," *IEEE Commun. Mag.* pp. 50-59, Jun. 1991.
- [9] Y. Ota et al., "Burst-Mode Compatible Optical Receiver With A Large Dynamic Range," *IEEE J. Lightwave Technol.*, vol. 8, no. 12, pp. 1897-1903, Dec. 1990.
- [10] Y. Ota et al., "DC-1Gb/s Burst-Mode Compatible Receiver for Optical Bus Applications," *IEEE J. Lightwave Technol.*, vol. 10, no. 2, pp. 244-249, Feb. 1992.
- [11] L. Lunardi et al., "A high speed burst mode optoelectronic integrated circuit photoreceiver using InP/InGaAs HBT's," *IEEE Photon. Technol. Lett.*, vol. 6, no. 7, pp. 817-818, Jul. 1994.
- [12] C. A. Eldering, "Theoretical determination of sensitivity penalty of burst-mode fiber optic receiver," *IEEE J. Lightwave Technol.*, vol. 11, pp. 2202-2214, Nov. 1993.
- [13] C. Su et al., "BER performance of digital optical burst-mode receiver in TDMA all optical multiaccess networks," *IEEE Photon. Technol. Lett.*, vol. 7, pp. 132-134, Jan. 1995.
- [14] C. Su et al., " Theory of Burst-Mode Receiver and Its Applications in Optical Multiaccess Networks," *IEEE J. Lightwave Technol.*, vol. 15, no. 4, pp. 590-606, Apr. 1997.



- [15] Y. Ota et al., "High-speed, Burst-mode, Packet-capable optical receiver and instantaneous clock recovery for optical bus operation," *IEEE J. Lightwave Technol.*, vol. 12, no. 2, pp. 325-331, Feb. 1994.
- [16] C. A. Eldering et al., "Digital burst mode clock recovery technique for fiber-optic systems," *IEEE J. Lightwave Technol.*, vol. 12, no. 2, pp. 271-278, Feb. 1994.
- [17] Y. Nagascako et al., "Fast timing extraction method for an optical passive bus," *Electron. Lett.*, vol. 26, no. 15, pp. 1168-1169, Jul. 1994.
- [18] M. Banu et al., "Clock recovery circuits with instantaneous locking," *Electron. Lett.* vol. 28, no. 23, Nov. 1992.
- [19] T. V. Muoi, "Receiver design for high speed optical fiber systems," *IEEE J. Lightwave Technol.* vol. LT-2, pp. 243-265, Jun. 1984.
- [20] Y. Ota et al., "Low-power, high-sensitivity 30Mb/s burst-mode/packet receiver for PON application," *OFC'94, Paper ThH-2*, pp. 210-212, San Jose, CA, Feb. 1994.
- [21] L. Lunardi et al., "High-speed burst-mode OEIC photoreceiver using InP/InGaAs heterojunction bipolar transistors," *Proc. OFC'94, San Jose, CA, paper TuH-2*, 1994.
- [22] P. M. Valdes, "Performance of optical direct receivers using noise corrupted decision threshold," *IEEE J. Lightwave Technol.*, vol. 13, no. 11, pp. 2202-2214, Nov. 1995.

- [23] C. Su et al., "Inherent transmission capacity penalty of burst-mode receiver for optical multiaccess networks," *IEEE Photon. Technol. Lett.*, vol. 6, pp. 664-667, May. 1994.
- [24] W. E. Stephens et al., "155.52 Mb/s data transmission on category 5 cable plant," *IEEE Commun. Mag.* pp. 62-69, Apr. 1995.
- [25] S. Ginzburg et al., "FDDI over unshielded twisted pairs," *IEEE Conference on Local Computer Networks*, Sep.
- [26] ANSI X3T12, "FDDI twisted pair physical layer medium dependent (TP-PMD)," *American National Standard*, 1994.
- [27] C. Su et al., "The MLT-N line code and multi-level burst-mode receiver for multiaccess local area networks," *IEEE Proc. SICON97*, pp. 371-385, Singapore, Apr. 1994.



CUHK Libraries



003598768